

**DEVELOPMENT OF ELECTROCHEMICAL-SURFACE PLASMON  
RESONANCE BIOSENSORS USING CONDUCTING POLYMERS**

**CHAMMARI POTHIPOR**

**DOCTORAL PROGRAM IN ELECTRICAL AND INFORMATION  
ENGINEERING  
GRADUATE SCHOOL OF SCIENCE AND TECHNOLOGY  
NIIGATA UNIVERSITY**

## ACKNOWLEDGEMENTS

The thesis has been accomplished with the assistance of Graduate School of Science and Technology, Niigata University, Niigata, Japan. I would like to express my deepest gratitude to Assoc. Prof. Dr. Kontad Ounnunkad, my supervisor at Chiang Mai University, for his kind recommendation, supervision, encouragement, thoughtfulness guidance and great support throughout my study.

I also would like to thank of gratitude to Prof. Dr. Akira Baba, my advisor at Niigata University, for his guidance, knowledge, opportunity to work in his laboratory, and many helpful suggestions. I am also thankful to Asst. Prof. Dr. Chutiparn Lertvachirapaiboon who gave me a lot of kindness advice, helps, useful discussions and sharing in both scientific and life experiences. I would like to thank Prof. Futao Kaneko, Prof. Keizo Kato, and Prof. Kazunari Shinbo for their supports, knowledge, and grateful kindness throughout my stayed in Japan. Moreover, I also like to thank all my colleagues of the research group at the Niigata University, Niigata, Japan for their friendship, helps, suggestions and joys in the laboratory. On the other hand, I also wish to express since appreciation to the examining committee for their valuable comments and suggestion.

I am grateful to The Ministry of Education, Culture, Sports, Science and Technology (MEXT 2015-2016) and double degree program (DDP) of Graduate School of Science and Technology, Niigata University, Niigata, Japan, for financial support during my Ph.D. program, great opportunities, invaluable experiences, knowledge, and facilities. The partial financial supports from Department of Chemistry, Faculty of Science and Graduate School, Chiang Mai University would also be acknowledged.

I would like to thank my seniors and my friends from the Chemistry Branch, the Department of Chemistry at Chiang Mai University, who has cheered me up, encouraged me, supported me and gave very thoughtful comments on my study and research.

Finally, I must extend special thanks to my family who have a great support to me and be a part of my success.

Chammari Pothipor

## ABSTRACT

The surface plasmon resonance (SPR)-based sensor offers direct, label-free, real-time, and quantifiable detection of the biomolecular interactions by measuring near a thin metal film surface or refractive index change. This technique provide opportunity for cost-effective and fast detection of the target molecules. In addition, electro-optical techniques combine electrochemical and optical data present more precise and detailed measurements that provide understandings of molecular function and structure. This thesis is divided in three result chapters. Chapter 2 have two sections to description the development of SPR and electrochemical-surface plasmon resonance (EC-SPR)-based biosensors for detection of immunoglobulin type G (IgG). In the first section, a simple and successful technique for constructing an electrochemical-surface plasmon resonance immunosensor (EC-SPR)-based on poly(2-aminobenzylamine)/graphene oxide (P2ABA/GO) is demonstrated. The GO composited with P2ABA is deposited on a gold surface by cyclic voltammetry CV technique with a potential range of -0.2 to 1.1 V for 2 cycles at a scan rate of 20 mV/s. After electropolymerization of the composite film, a shift of SPR dip is observed. The enhancement of IgG detection on P2ABA/GO/gold film is obtained compared with P2ABA film. The GO has a larger number of functional groups for example, hydroxyl, carboxylic, and epoxides, than the gold electrode. To interact with the target molecule, the surface functionality of GO, which contains epoxy/hydroxyl groups in the basal plane and carboxylic acid groups at the edge plane, can be used. The concentration dependence exhibits a linear relationship with human IgG in the range from 1.0 to 10  $\mu\text{g/mL}$  and the lowest detection limit (LOD) of 0.95  $\mu\text{g/mL}$ , suggesting good device performances in the detection of human IgG.

In section 2, the incorporation of graphene oxide-poly(3,4-ethylenedioxythiophene)/poly(styrenesulfonate) (GO/PEDOT/PSS) thin film on gold-coated high reflective index substrate is employed IgG by EC-SPR technique. The EC-SPR immunosensors are strong bioanalysis instruments that are label-free and have high stability, specificity, and sensitivity for measuring antigens binding to antibodies fixed on the SPR sensor surface. The GO/PEDOT/PSS film is prepared by in situ electropolymerization on a gold electrode and subsequently chemical modified carboxylic terminal group of GO by surface-confined ester reaction of EDC/NHS. The human IgG selectively reacted with the functionalized substrate by covalent binding of amide coupling reaction. The number of binding site for immunoreaction of the GO/PEDOT/PSS film is increased by applied potential as the incorporate polymer film is swollen and surface area of the film is increased under doping. The significant increase in the binding of human IgG molecules on the functionalized substrate state is observed when the applied potential is increased. In compared to an open circuit and applied potentials in the ranging from -1.0 to 0.5 V, the EC-SPR immunosensor has the highest sensitivity when applied potential at 0.5 V. The SPR intensity exhibits linearity in the concentration of IgG from 1.0 to 10  $\mu\text{g/mL}$  with a LOD of 0.35  $\mu\text{g/mL}$ .

In addition, Chapter 3 has two parts. The first part of this chapter described a facile and label-free approach for constructing high-sensitivity, GO-based TSPR biosensors with high precision and accuracy over important analyte measurement ranges. The binding phenomena between proteins IgG and anti-IgG/GO films is detected using the TSPR method. TSPR is a surface-sensitive optical technique for detecting biomolecular interactions close to

sensor interfaces. It provides real-time and label-free analytical detection by the changes of interfacial refractive index associated with any specific binding interface after biomolecule immobilized on a sensor surface. The application of TSPR in biosensors offers a unique potential because to its rapid and simultaneous analysis without labeling, accurate detection, and low LOD. In this section 2, we demonstrate transmission surface plasmon resonance-imaging (TSPR-i) with a microfluidic 3-channel cell. Silver nanoparticles (AgNPs) are deposited with poly (diallyldimethylammonium chloride) (PDADMAC) and poly (sodium 4-styrenesulfonate) (PSS) using layer-by-layer (LbL) technique on gold thin film grating/substrate surfaces. TSPR-i technique is used to study the effect of localized surface plasmon resonance (LSPR) from plasmonic AgNPs on the gold-grating/dielectric interface for the signal enhancement of creatinine detection. After the deposition of AgNPs on the gold grating substrate, a decrease of TSPR-i intensity is observed. 10 mM creatinine solution is injected into the 3-channel microfluidic cell for 1 h. The brighter TSPR image is obtained after the injection of creatinine on the AgNPs/gold grating system. UV-vis absorption spectroscopy is used to study a 5-bilayer AgNPs/PDADMAC film on 10 layers of PDADMAC/PSS intermediate layers on BK7 glass slides before and after injection of creatinine. The AgNPs/PDADMAC film with a peak wavelength of 420 nm is deposited onto the surface of a PDADMAC/PSS multilayer. The plasmon absorption band of AgNPs at 420 nm reduced after injection of 10 mM creatinine. The creatinine sensor has a high sensitivity for creatinine measurement and a linear calibration range of 0.1 to 20 mM. On the TSPR-i system, a facile and cost-effective approach for label-free, real-time, and high-sensitivity has been established, which might be helpful for clinical applications.

In this chapter 4, we constructed new approach for creatinine assay on polypyrrole (PPy) film utilizing SPR method. The change of SPR reflectivity induced by adsorption of the product of AgNPs and creatinine on polymer film. The creatinine at different concentrations is mixed with 20 ppm of AgNPs solution before injection of the product solution in a SPR sensor. The SPR reflectivity change on the substrate by the mixed solution with AgNPs is increased with increasing creatinine concentration whilst without AgNPs, no change is observed. Furthermore, the interaction between polymer film and product will be studied. The adsorption of AgNPs on the PPy film with creatinine increased the shift in SPR reflectivity. The SPR reflectivity increased with increasing creatinine content after adding the mixed solution to the PPy/gold substrate. The performance of the creatinine sensor is compared to that of three SPR sensor platforms: PPy film, PPy film with AgNPs, and PPy film by aggregated AgNPs. When compared to a substrate without aggregated AgNPs, the SPR sensor with aggregated AgNPs enhanced to about 4 folds, and the LOD is 0.19  $\mu$ M. The developed technique has the potential to be beneficial in biomedical applications.

## CONTENTS

	<b>PAGE</b>
ACKNOWLEDGMENTS	b
ABSTRACT	c
CONTENTS	g
LIST OF FIGURES	l
LIST OF TABLES	p
LIST OF ABBREVIATIONS AND SYMBOLS	q
<b>CHAPTER 1 INTRODUCTION</b>	<b>1</b>
1.1 BACKGROUND	1
1.2 SENSOR AND BIOSENSOR	2
1.3 CLASSIFICATION OF BIOSENSORS	3
1.4 OPTICAL BASED BIOSENSOR	4
1.4.1 COLORIMETRIC SENSORS	5
1.4.2 SURFACE PLASMON RESONANCE BASED BIOSENSORS	6
1.4.3 TRANSMISSION SURFACE PLASMON RESONANCE BASED SENSORS	9
1.4.4 ELECTROCHEMICAL-SURFACE PLASMON RESONANCE SPECTROSCOPY	11
1.5 MATERIALS FOR SPR SENSOR	13
1.5.1 CONDUCTING POLYMER	13
1.5.2 GRAPHENE OXIDE BASED SPR BIOSENSORS	15
1.5.3 METAL NANOPARTICLES	16
1.6 BIOMARKERS	17
1.6.1 IMMUNOGLOBULIN G	17

## CONTENTS (CONTINUED)

	<b>PAGE</b>
1.6.2 CREATININE	17
1.7 CHARACTERIZATION TECHNIQUES	17
1.7.1 ATOMIC FORCE MICROSCOPY	17
1.7.2 UV–VIS SPECTROSCOPY	18
1.7.3 IMAGING TECHNOLOGY	19
1.8 OBJECTIVES	19
1.9 SCOPE OF THESIS	20
1.10 REFERENCES	22
<b>CHAPTER 2</b>	
<b>SURFACE PLASMON RESONANCE BASED BIOSENSORS FOR DETECTION OF HUMAN IMMUNOGLOBULIN G</b>	26
2.1 INTRODUCTION	26
2.2 EXPERIMENTAL DETAILS	29
2.2.1 CHEMICALS AND MATERIALS	29
2.2.2 EC-SPR INSTRUMENTATION	29
2.3 A GRAPHENE OXIDE/POLY(2-AMINOBENZYLAMINE)-BASED SURFACE PLASMON RESONANCE IMMUNOSENSORS	30
2.3.1 CONSTRUCTION OF GO/P2ABA/GOLD-BASED IMMUNOSENSOR	30
2.3.2 RESULTS AND DISCUSSION	31
2.3.3 CONCLUSION	37



## CONTENTS (CONTINUED)

	<b>PAGE</b>
2.4 ELECTROCHEMICAL SURFACE PLASMON RESONANCE IMMUNOSENSOR-BASED GRAPHENE OXIDE/POLY (3,4 ETHYLENEDIOXYTHIOPHENE)/ POLY (STYRENE SULFONATE) THIN FILM	38
2.4.1 FABRICATION OF GO/PEDOT/PSS ELECTRODE	38
2.4.2 PREPARATION OF EC-SPR BIOSENSOR	38
2.4.3 REULTS AND DISCUSSION	40
2.4.3.1 FABRICATION AND DESCRIPTION OF GO/PEDOT/PSS FILM	40
2.4.3.2 STRUCTURE OF EC-SPR BIOSENSOR BASED ON GO/PEDOT/PSS SUBSTRATE	43
2.4.3.3 THE ASSAY OF IgG BY GO/PEDOT/PSS ELECTRODE	44
2.4.3.4 KINETIC STUDY OF IMMUNOREACTION AT ELECTRODE SURFACE	49
2.4.4 CONCLUSION	53
2.4.5 REFERENCES	54
<b>CHAPTER 3</b>	
<b>TRANSMISSION SURFACE PLASMON RESONANCE BASED SENSORS</b>	<b>56</b>
3.1 A GRAPHENE OXIDE-BASED TRANSMISSION SURFACE PLASMON RESONANCE BIOSENSOR FOR DETECTION OF HUMAN IgG	56

## CONTENTS (CONTINUED)

	<b>PAGE</b>
3.1.1 INTRODUCTION	56
3.1.2 EXPERIMENTAL FEATURES	57
3.1.2.1 CHEMICALS AND MATERIALS	57
3.1.2.2 INSTRUMENTATION	58
3.1.2.3 SUBSTRATE PREPARATION	58
3.1.2.4 FABRICATION OF IMMUNOSENSOR	59
3.1.2.5 CONSTRUCTION OF 11-MERCAPTOUNDECANOIC ACID (11-MUA) FOR THE ASSAY OF HUMAN IgG	60
3.1.3 RESULTS AND DISCUSSION	61
3.1.4 CONCLUSION	64
3.2 TRANSMISSION SURFACE PLASMON RESONANCE IMAGING FOR DETECTION OF CREATININE	65
3.2.1 INTRODUCTION	65
3.2.2 EXPERIMENTAL	66
3.2.2.1 INVESTIGATION OF SYSTEM FOR TSPR IMAGE ACQUIREMENT	66
3.2.2.2 TSPR SUBSTRATE PREPARATION	66
3.2.3 RESULTS AND DISSCUSSION	67
3.2.4 CONCLUSION	70
3.3 REFERENCES	71

## CONTENTS (CONTINUED)

	<b>PAGE</b>
<b>CHAPTER 4</b>	
<b>ELECTROCHEMICAL-SURFACE PLASMON RESONANCE BASED SENSOR FOR DETECTION OF CREATININE</b>	<b>73</b>
4.1 INTRODUCTION	73
4.2 EXPERIMENTAL METHODS	74
4.2.1 CHEMICALS AND MATERIALS	74
4.2.2 EC-SPR EQUIPMENT	74
4.2.3 CONSTRUCTION OF POLYPYRROLE ELECTRODE-BASED SPR SENSOR FOR THE ASSAY OF CREATININE	75
4.3 RESULTS AND DISCUSSION	76
4.3.1 UV-VIS ABSORPTION STUDIES OF AgNPs-CREATININE STRUCTURE	76
4.3.2 FABRICATION AND CHARACTERIZATION OF POLYPYRROLE ON GOLD FILM	77
4.3.3 THE DETECTION OF CREATININE BY SURFACE PLASMON RASONANCE TECHNIQUE	78
4.4 CONCLUSION	84
4.5 REFERENCES	85
<b>CHAPTER 5</b>	
CONCLUSION	86
APPENDICE	89
LIST OF PUBLICATIONS	90
CURRICULUM VITAE	94

## LIST OF FIGURES

	<b>PAGE</b>
Figure 1.1 The basic mechanisms and components of biosensors for use in clinical diagnoses	4
Figure 1.2 Overview of existing technologies for colorimetric virus detection	6
Figure 1.3 Fundamentals of surface plasmon resonance (SPR) sensor	8
Figure 1.4 Direct label-free detection based SPR sensor and the SPR sensogram	9
Figure 1.5 the experimental device used to measure the transmission spectrum	11
Figure 1.6 Schematic diagram of EC-SPR	12
Figure 1.7 Chemical structures of the various conducting polymers	14
Figure 1.8 Jablonski-type energy level diagram	18
Figure 2.1 SPR setup and step of SPR immunosensor for IgG detection	31
Figure 2.2 (a) CV curve for 2 cycles of electropolymerization of P2ABA (b) CV curve for electropolymerization of GO/P2ABA for 2 cycles (c) CV curve of P2ABA and GO /P2ABA in gold film scan in solution of PBS (d) SPR angular reflectance curve of bare gold substrate, Au/P2ABA and Au/GO/P2ABA (e) SPR kinetics of Au / P2ABA and Au/GO/P2ABA, used to detect 10 $\mu\text{g}/\text{ml}$ of IgG	33
Figure 2.3 (a) CV curves of Au/GO/P2ABA film at different scan rates from 20 to 100 mV/s in PBS solution (b) and the plots of anodic peak current with scan rate	34
Figure 2.4 SPR response to detect human IgG (10 $\mu\text{g}/\text{mL}$ ) during the construction of Au/GO/P2ABA-based immunosensor	35
Figure 2.5 SPR kinetics as a function of IgG concentration. (a) P2ABA, (b) GO/P2ABA and (c) two calibration curves for the detection of IgG and GO	36

## LIST OF FIGURES (CONTINUED)

	<b>PAGE</b>
Figure 2.6 Schematic diagram of the construction of GO/PEDOT/PSS-based immunosensor for the detection of human IgG	39
Figure 2.7 CV curves of electropolymerization of (a) PEDOT/PSS and (b) GO/PEDOT/PSS and (c) films gold coated SPR chip	41
Figure 2.8 (a) SPR reflectivity curves of bare, PEDOT/PSS film, and GO/PEDOT/PSS film on gold SPR substrates in contact with 0.01 M PBS solution. (b) CV curves of bare, PEDOT/PSS film, and GO/PEDOT/PSS film on gold SPR substrates in contact with 0.01M PBS solution. (c) SPR reflectivity curves of GO/PEDOT/PSS film with different applied constant potentials and open circuit. (d) UV–vis spectra of GO, PEDOT/PSS, and GO/PEDOT/PSS films	42
Figure 2.9 (a) Sensorgram of a GO/PEDOT/PSS-based biosensor during construction and assay 10 $\mu\text{g/mL}$ IgG with used potential at 0.50 V. The kinetic reaction of SPR during PEDOT/PSS formulation without (b) and with GO (c) after injection of the EDC/NHS mixture as a coupling reagent for 5 min and rinsing with PBS buffer.	44
Figure 2.10 (a) Graph of reflectivity change as a function of IgG concentration for immunosensors based on 3-MPA, PEDOT/PSS, GO, and GO/PEDOT/PSS with no applied potential and (b) graph of reflectance change with IgG concentration for the proposed immunosensor based on GO/PEDOT/PSS at different constant applied potentials and in open circuit	48
Figure 3.1 showing construction of gold gratings	58
Figure 3.2 Schematic representation of the fabrication of GO based immunosensor for the detection of human IgG	60
Figure 3.3 Schematic representation of the fabrication of 11-MUA based immunosensor for the detection of human IgG	61

## LIST OF FIGURES (CONTINUED)

	<b>PAGE</b>
Figure 3.4 The TSPR response of gold-coated DVD grating substrate as a function of incident	62
Figure 3.5 TSPR responses during the fabrication of 11-MUA-based immunosensor for detection of human IgG (10 $\mu\text{g}/\text{mL}$ ) and (b) TSPR responses during the fabrication of GO-based immunosensor for detection of human IgG (10 $\mu\text{g}/\text{mL}$ )	63
Figure 3.6 Graph of human IgG concentration and progression of TSPR response during human IgG binding to human IgG-GO compared with human IgG-MUA SAM system	64
Figure 3.7 Photograph of the T-SPR imaging system	66
Figure 3.8 Schematic diagram representing the gold-coated grating/PDADMAC/PSS (10 bilayers)/PDADMAC/AgNPs (5 bilayers)/PDADMAC/PSS layer-by-layer (LBL) film assembled for the creatinine detection on gold grating substrate	67
Figure 3.9 TSPR spectra of a gold-coated imprinted grating substrate and gold-coated grating/ PDADMAC/PSS (10 bilayers) / PDADMAC/AgNPs (5 bilayers) / PDADMAC/PSS at incident angles of $0^\circ$ to $40^\circ$	68
Figure 3.10 The TSPR response of a gold-coated grating substrate (black), after the deposition of PDADMAC/AgNPs on PDADMAC/PSS film (red), and after the injection of creatinine on the gold-coated grating/PDADMAC/PSS/AgNPs-PDADMAC/PSS (green)	69
Figure 3.11 (a) The TSPR imaging and (b) The intensity of TSPR imaging of PBS	70
Figure 4.1 Schematic diagram of the construction of SPR creatinine sensor using AgNPs on PPy/gold electrode	75

## LIST OF FIGURES (CONTINUED)

	<b>PAGE</b>
Figure 4.2 (a) UV-Vis absorption spectrum of AgNP, creatinine and AgNPs-creatinine over time after mixing (b) Delta LSPR at 400 nm from 0 to 60 minutes with time, and (c) $A_{550\text{nm}}/A_{400\text{nm}}$ as a function of time, from 0 to 60 minutes after mixing AgNP and creatinine	77
Figure 4.3 (a) CV curves during the electropolymerization of PPy film onto gold coated SPR chip for 3 cycles and SPR kinetic property during the electropolymerization of PPy for 3 cycles (inset), (b) SPR reflectivity curves of bare gold and PPy film/gold substrate	78
Figure 4.4 SPR response in AgNPs/creatinine (after the mixture 30 min) AgNPs/creatinine (after 0 min), AgNPs, and, PBS solution on the PPy/gold electrode, (b) AgNPs/creatinine (after the mixture 30 min), and (c) Three linear curves for the assay of creatinine present and absent AgNPs; the black, red, and green lines related to AgNPs/creatinine (after the mixture 30 min), AgNPs/creatinine (after the mixture 0 min), and creatinine solution, respectively.	80
Figure 4.5 Interference study	82
Figure 4.6 (a) SPR reflectivity properties of (a) AgNPs and (b) AgNPs-creatinine (0.5 mM) at constant applied potentials of $-0.3$ , $0.3$ and $0.5$ V and at an open circuit potential	83

## LIST OF TABLES

	<b>PAGE</b>
Table 2.1. Comparison of the sensitivity of all immunosensors under different constant potentials	46
Table 2.2 shows the $k_a$ and $k_d$ values determined from the designed GO/PEDOT/PSS biosensor at different IgG concentrations.	51
Table 2.3 $k_a$ and $k_d$ values obtained from our proposed GO/PEDOT/PSS based immunosensor at different concentrations of human IgG	51
Table 2.4 Freundlich's constant for human IgG binding of the GO/PEDOT/PSS-based immunosensor	53
Table 4.1 The PPy, PPy/AgNPs and PPy/aggregated AgNPs based sensor with different creatinine concentrations.	82
Table 4.2 $k_a$ and $k_d$ obtained from our proposed PPy/aggregated AgNPs based sensor at 0.5 mM creatinine under electrochemical control	84



## LIST OF ABBREVIATIONS AND SYMBOLS

AFM	Atomic force microscope
ATR	Attenuated total internal reflection
AuNPs	Gold nanoparticles
AgNPs	Silver nanoparticles
Anti-IgG	Anti-human immunoglobulin G
AA	Ascorbic acid
AgNPs	Silver nanoparticles
Ag/AgCl	Silver/silver chloride
Amp	Amperometry
AuNPs	Gold nanoparticles
CE	Counter electrode
CNT	Carbon nanotubes
CPs	Conducting polymers
CV	Cyclic voltammetry
DPV	Differential pulse voltammetry
2D	Two-dimensional
EC	Electrochemical
EA-HCl	Ethanolamine hydrochloride
EDC	1-ethyl-3-(3-dimethylaminopropyl)-carbodiimide hydrochloride
EIS	Electrochemical impedance spectroscopy
fM	Femtomolar
GCE	Glassy carbon electrode
Glu	Glucose
GO	Graphene oxide
GP	Graphene
g	Gram
h	Hour

## LIST OF ABBREVIATIONS AND SYMBOLS (CONTINUES)

IUPAC	International union of pure and applied chemistry
IgG	Immunoglobulin G
ITO	Indium tin oxide
L	Liter
LSPR	Localized surface plasmon resonance
LSV	Linear sweep voltammograms
LOD	Limit of detection
mg	Milligram
mm	Millimeter
mV	Millivoltage
mL	Milliliter
min	Minute
mM	Millimolar
MWNTs	Multiwalled carbon nanotubes
NP	Nanoparticle
NHS	N-Hydroxysuccinimide
PEDOT	poly(3,4-ethylenedioxythiophene) polystyrene sulfonate
PBS	Phosphate buffered saline
PSS	Poly(styrene sulfonate)
PPy	Polypyrrole
SEM	Scanning electron microscope
SPR	Surface plasmon resonance
$\mu$ L	Microliter
$\mu$ g	Microgram
$\mu$ M	Micromolar

## LIST OF ABBREVIATIONS AND SYMBOLS (CONTINUES)

nm	Nanometer
pM	Picomolar
PCR	Polymerase chain reaction
rGO	Reduced graphene oxide
RE	Reference electrode
SWV	Square wave voltammetry
TEM	Transmission electron microscopy
TSPR	Transmission Surface plasmon resonance
TSPR-i	Transmission Surface plasmon resonance imaging
UA	Uric acid
V	Voltage
WE	Working electrode
°C	Degree Celsius
%	Percent
$\pi$	Pi
$\lambda$	Wavelength
$I$	Current
$I_{pa}$	Anodic peak current
$I_{pc}$	Cathodic peak current
E	Potential
$\Delta$	Delta
$\Omega$	Ohm
v	Scan rate

# CHAPTER 1

## INTRODUCTION

### 1.1 BACKGROUND

The specific-biomarker detection is an increasingly important clinical tool for the treatment and differential diagnosis of various diseases [1]. Therefore, the capability to assay biomarkers in real-time, rapidly, and accurately is of much importance in clinical analysis. Biosensors have been one of the most attractive analytical methods for the detection of biomarkers. Biosensors can measure the level of biomarkers with high selectivity and sensitivity due to specific reactions via pair of enzyme and substrate or of antibody-antigen. Thus, these biodevices can transform the chemical interaction of high specific analytes into an electrical or optical signal by a transducer. The surface plasmon resonance (SPR) method has been widely applied to monitor the interaction between two binding biomolecules and detect pathogens including viruses and bacteria, allergens, toxins, antigens, antibodies, and nucleic acids. The SPR-based sensor offers direct, label-free, real-time, and quantifiable detection of interactions by measuring near a thin metal film surface or refractive index change and provides an opportunity for cost-effective and fast detection of the target molecules. SPR sensors have been used for medical diagnosis. By the combination of electrochemical and optical techniques in the biosensors, superior devices have been achieved with real-time measurement and better device performances such as higher sensitivity and lower limit of detection. Moreover, nanomaterials and nanostructures for the construction of the devices will also offer improvement of device performances.

In this work, we will develop the SPR, EC-SPR, TSPR, TSPR image-based biosensors for sensitive detection of biomarkers. This method has been broadly considered as a potential analysis device due to its high sensitivity caused by changes in the degree of the probe surface. Compared to biochemical assays such as ELISA and RIA, EC-SPR biosensors provide more benefits such as do not require a labeling process, reducing the complexity of measurement, and real-time analysis of surface interactions, low-cost analysis, and the regeneration of the sensor surface. Our work, therefore, aims to fabricate high-performance SPR, EC-SPR, TSPR, and TSPR image biosensors based on nanocomposites. The proposed SPR, EC-SPR, TSPR, and TSPR image sensing system will provide higher sensitivity and lower limits of detection.

## **1.2 SENSOR AND BIOSENSOR**

A biosensor is an analytical tool consisting of a biosensor element connected to a physicochemical probe. Due to the specificity of biomolecule interactions, biosensors can be used to analyze complex substrates, including serum, blood, plasma, milk, urine, and culture media, which usually require minimal preparation of samples. There are three main components of biosensors including a biological recognition element, a transducer, and a signal processing system. Biological receptors generally consist of immobile biological components that can be monitored for specific target analyses [2]. This biological component is mainly composed of antibodies, nucleic acids, cells, and enzymes. The interaction between the biological receptor and the analyzed substance causes chemical changes, such as the

release of heat, new chemical production, electron flow, and changes in pH or mass. Biochemical signals are changed into electrical signals by transducers.

### **1.3 CLASSIFICATION OF BIOSENSORS**

Different types of biosensors have been established including amperometric, potentiometric, piezoelectric, colorimetric, and optical biosensors. These have been employed in food and water analysis and medicinal processes due to their demands for sensitivity, specificity, speed, and accuracy of measurements [3]. Optical biosensors are related to changes in mass, concentration, or amount of molecules with direct changes in optical properties [4]. Optical detection using SPR biosensors has gained popularity due to its high detection speed, high specificity, high sensitivity, and real-time analysis capabilities [5, 6]. The various types of biosensors are shown in Figure 1.1.

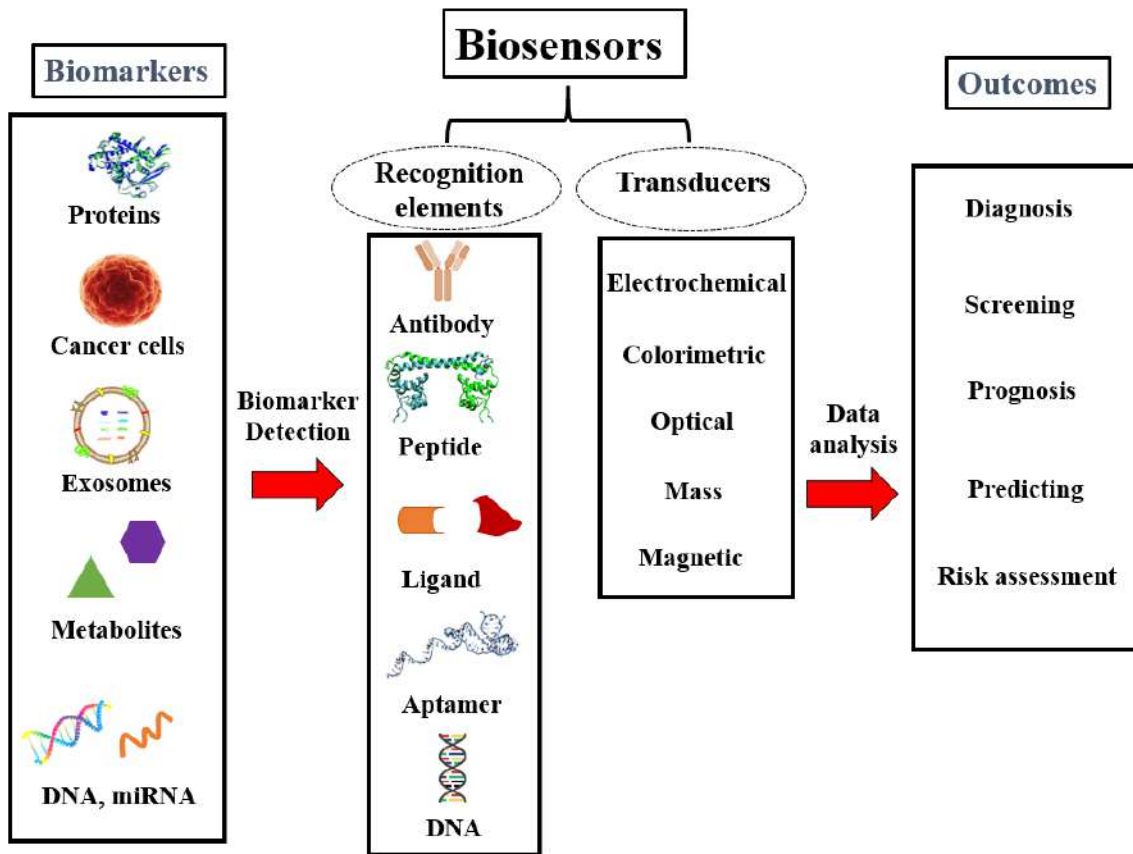


Figure 1.1 The basic mechanisms and components of biosensors for use in clinical diagnoses.

#### 1.4 OPTICAL BASED BIOSENSOR

Optical biosensor has developed and are used in many significant fields such as biological safety, food safety, environmental monitoring, and remedy [7]. In medicine, an optical transducer is recognized in both medical diagnostics and medical applications. The term "optrode" is a combination of the word's "light" and "electrode". This technique of transduction is applied in many categories of biosensors due to different kinds of spectroscopy such as fluorescence, absorption, Raman, SERS, phosphorescence, dispersion,

and refraction spectroscopy [8]. These transfer methods can measure different properties of analyte/target. Optical biosensors can offer real-time and label-free detection. The SPR is the most popular method. It appears that sensors based on optics have received attention in research and applications in the study of biosensors.

#### **1.4.1 COLORIMETRIC SENSORS**

Colorimetric sensors are becoming increasingly popular due to their ease to use, high accessibility, low cost, selective and sensitive response to many analytes. A colorimetric sensor is a type of optical sensor that changes color when affected by outside stimuli. Some change in the chemical or physical environment can be considered this trigger. Thus, it is necessary to detect changes in environmental characteristics when designing a colorimetric sensor [9]. Colorimetric is a distinctive technique used for routine food and clinical analysis samples. Gold nanoparticles (AuNPs) have become very attractive color indicators in colorimetric analysis due to their uncomplicatedness [10].



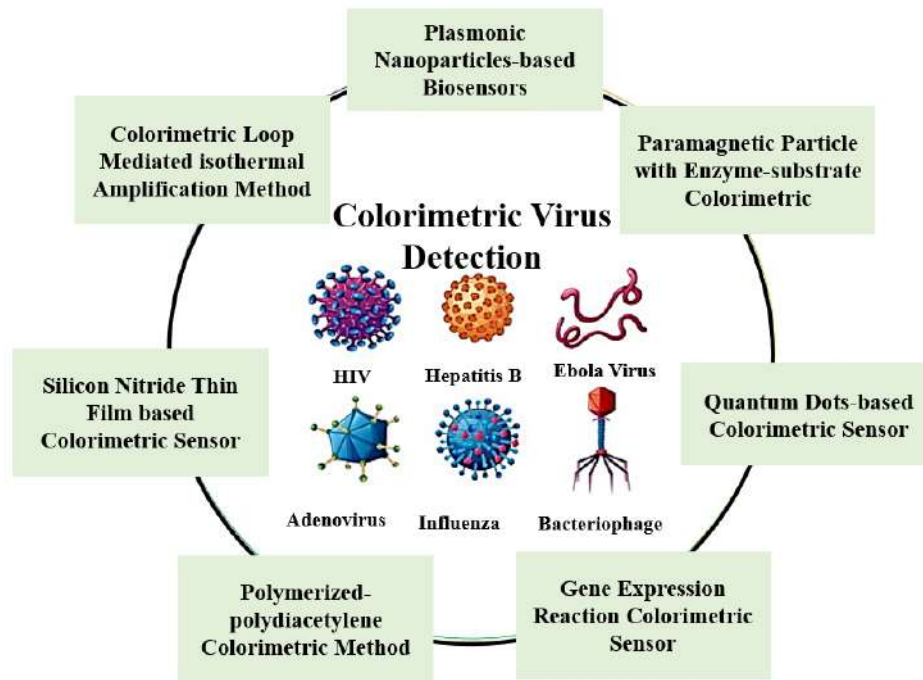


Figure 1.2 Overview of existing technologies for colorimetric virus detection [11].

#### 1.4.2 SURFACE PLASMON RESONANCE BASED BIOSENSORS

SPR is defined as the oscillation of the charge mass at the interface between the metal and the dielectric. The electromagnetic field of the surface plasmon wave (SPW) at the metal-dielectric interface has a maximum intensity and can reduce the emitted wave (EW) exponentially in both media, as well as has a direction of propagation that varies at VIS and NIR (100 to 600 nm) [12]. Grating couplers, prism couplers, or metal dielectric waveguides are configurations used to excite surface plasmons, but the former describes the most common method of excitation of plasma by attenuated total reflection (ATR). In the Kretschmann configuration, light waves are completely reflected in the medium between a highly refractive prism coupler (usually glass) and a thin metal layer (usually 50 nm thick

gold or silver). Kretschmann geometry is also applicable for detection and biosensing applications. The reflected light excites the surface plasmons of the metal film, causing EW or SPW to penetrate the metal layer (Figure 1.3).

There are many researchers studied the SPR technique for analytical fields such as the food science, pharmaceutical approaches, doping analysis, proteomics and genomics, and environmental monitoring. In a typical SPR test, an interacting molecule called a "ligand" binds to the sensor surface, while another molecule called an "analyte" is transported to the surface in a continuous flow complete a complex microfluidic structure. The SPR biosensor consists of a gold-coated glass section, providing a platform for a range of specialized surfaces designed to optimize the binding of biomolecules, including proteins, nucleic acids, lipids, carbohydrates, inorganic compounds, and even whole cells. The gold layer in the biosensor enables the generation of SPR events that effectively detect mass variations in the water layer near the surface of the biosensor by measuring changes in the refractive index of the polarization light beam incident (Figure 1.3) [13]. The resulting data provides real-time quantitative information on binding specificity, active concentrations of the molecule in the sample, kinetics, and affinity of binding patterns [14].

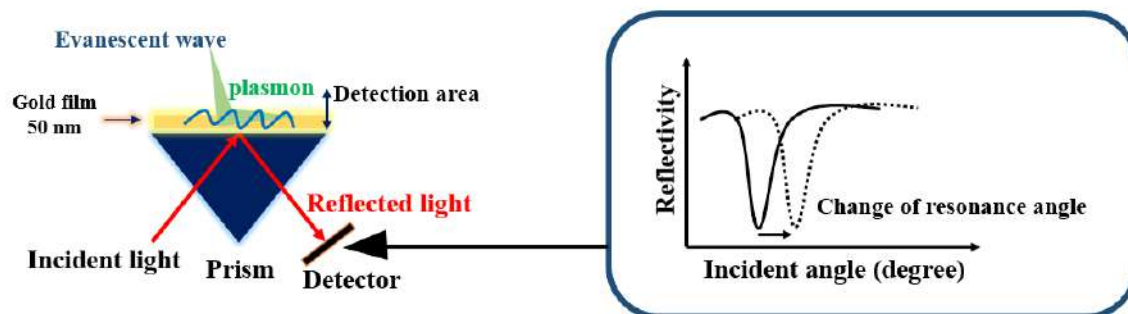


Figure 1.3 Fundamentals of surface plasmon resonance (SPR) sensor.

Depending on the wavelength time or resonance angle shift at which water immersion is observed will produce the sensor graph (Figure 1.4), the number of species adsorbed after the initial injection of the buffer of basis can be determined and kinetic studies of biomolecular interactions can be determined. The sensor surface should be conditioned with an appropriate buffer solution to initiate each measurement. It is important to have a stable baseline first. After injection of the analyte, the binding phase begins and the receptors on the surface of the sensor capture the target molecule. Upon injection of the base, the dissociation of target molecules and non-specifically bound compounds from the surface begins. This step is important to perform multiple tests using the same sensor surface [15].

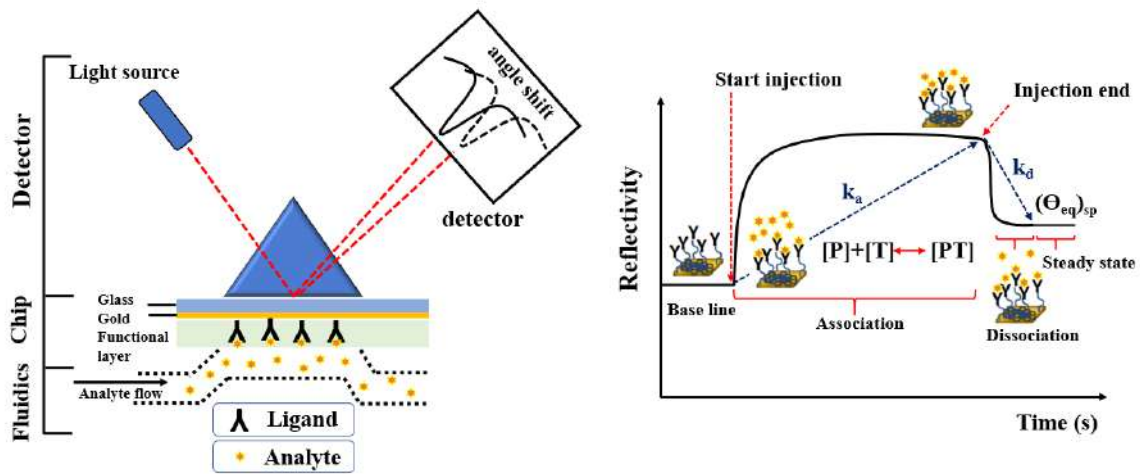


Figure 1.4 Direct label-free detection based SPR sensor and the SPR sensogram.

### 1.4.3 TRANSMISSION SURFACE PLASMON RESONANCE BASED SENSORS

The TSPR technique is important in light transmission via nanopore arrays because the amplitudes and locations of these increased transmission peaks are sensitive to changes in refractive index near the surface, providing molecule binding events to be detected [16, 17]. Transmission peaks obtained at the level of an arrangement of nanosits and nanopores are used to construct sensors. These sensors outperform traditional SPR detection methods. Sensors that detect the reduction in reflected light intensity, for example, may be strongly influenced by noise. Advanced transmission monitoring improves the signal-to-noise ratio by creating bright spots on a dark field. Alternatively, these transmission data are measured in a straightforward linear way by aligning the light source, sample, and detection system on a straight line. This eliminates the need for exact angular alignment, which is required in typical SPR sensors. One of the major drawbacks of nanostructured sensors is the

requirement for complex high-resolution processing in order to produce sub-wavelength topographic features [18].

Gratings are basic nanostructured surfaces that have been employed in surface plasmons for biosensing. These sensor structures are based on specular reflection or directly measure the diffraction peaks produced on the surface of the stamped or coupled to the prism. [19]. In this thesis, a facile platform based on affordable and widely available diffraction gratings is employed to conduct transmission-based detection using surface plasmons' exceptional optical transmission. A thin gold layer is applied to the transparent diffraction grating, which is then bombarded with p-polarized white light. In a limited wavelength range, improved light transmission is found, which matches to the conditions for generating surface plasmons in the gold-air interface. It is recently discovered that nanoscale holes aren't necessary to improve transmittance and that the peak of transmitted light may be seen through a continuous metal sheet [20]. The experimental system employed to measure the transmission spectrum through the grating substrate and the transmission spectrum of the gold film with a thickness of 45 nm using s-polarized light and p-polarized light at  $\theta = 50^\circ$  as shown in Figure 1.5.

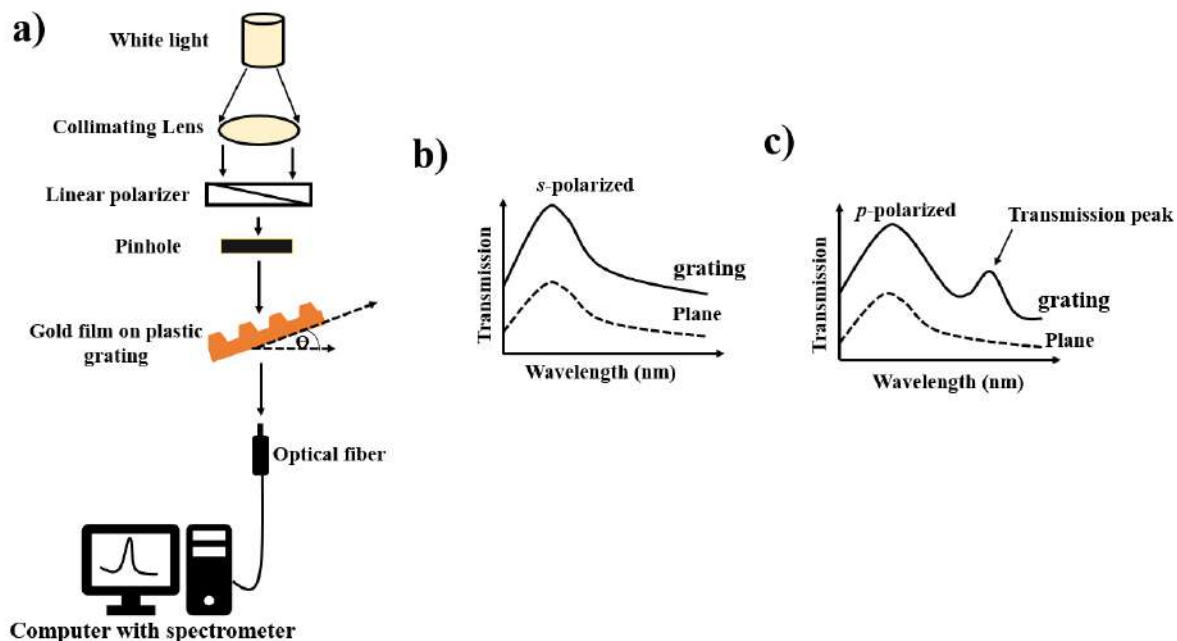


Figure 1.5 (a) shows the experimental device used to measure the transmission spectrum through a grating sample and the transmission spectrum of a 45 nm thick gold film with  $\theta = 50^\circ$ , (b) light s-polarized and (c) p-polarized light in the a-plane (dotted line) and grating (solid line).

#### 1.4.4 ELECTROCHEMICAL-SURFACE PLASMON RESONANCE SPECTROSCOPY

The purpose of the development of EC-SPR is to analyze the small changes in the electrostatic field on the electrode surface and to study the structure and activity of the redox active structure (Figure 1.6) [21]. In this structure, an electrode composed of three electrodes is placed together in the SPR system for study the interaction between chemical changes and electrical energy. In a triple electrochemical cell, a potential difference is used between the counter electrode and the working electrode, while measuring the current flowing in the

circuit due to the electrochemical reaction. The potential needed to drive the working electrode is given with respect to the reference electrode, representing the potential with respect to a known and stable solution.

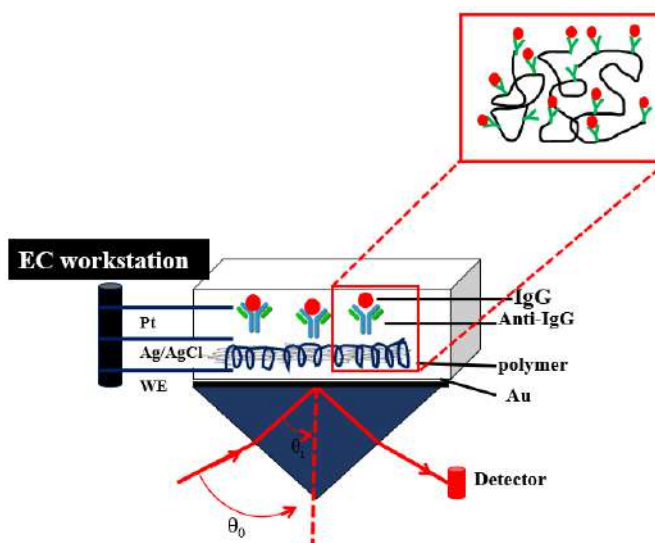


Figure 1.6 Schematic diagram of EC-SPR.

In the EC-SPR system, the working electrode is applied to control the potential and electric field of the interface. The potential of the working electrode generally oscillates between two potentials at a constant rate (cyclic voltammetry (CV)). The generated current contains two components; the Faraday component and the non-Faraday component related to the electrochemical reaction due to the charging of the interface capacitance. This is used in EC-SPR to greatly expand the available application space of SPR, allowing SPR to be used to the study of charge transfer procedures, potential control molecular adsorption, enzymatic processes, anode extraction, and characterization of electrochemical sensors [22].

## **1.5 MATERIALS FOR SPR SENSOR**

### **1.5.1 CONDUCTING POLYMER**

Conductive polymer (CP) is a material that has been exposed for more than 20 years. An electrical conductivity, optical properties, and chemical and biochemical properties have attracted attention. Due to biocompatibility, convenient construction, and low cost, conductive polymer-based biosensors provide an ideal platform for various detection applications [23]. CP has been widely used as an easy-to-construct, biocompatible matrix material for various analytes. CP-based biosensors directly immobilize probes (such as oligonucleotides or antibodies and enzymes) on polymeric membranes simply by mixing probes with monomers prior to electropolymerization. In this quick and easy process, the intercalation of the CP matrix and the unlabeled molecules is very important for the immobilization of the probe [24]. Typical samples of conductive polymers such as poly (3,4-ethylenedioxythiophene) (PEDOT), polyaniline (PANI), polypyrrole (PPy), and their derivatives have been considered extensively. Among conductive polymers, PEDOT is widely used in many sensor applications due to its high conductivity, stability at high temperatures in air, and resistance to humidity. PEDOT can be polymerized from 3,4-ethylenedioxythiophene (EDOT) monomer by chemical or electrochemical processes. The polystyrene sulfonate (PSS) acts as a template during the charge balancing and polymerization counter ion process, thus keeping the PEDOT cationic segments dispersed in the aqueous medium [25]. In addition, PPy have been greatly studied because of their high conductivity, ease to synthesis using electrochemical and chemical techniques, and



environmental stability to water and air. The EC-SPR is monitored by PPy nano film [26]. The P2ABA has received significant consideration in biosensor application due to its high conductivity, simple and nanoscale controlled for electropolymerization on the electrode surface. The P2ABA has an amine group in the structure, which can form van der Waals and electrostatic interactions with the carboxylic group in GO structure [27]. The chemical structures of the various CPs are used in this work as show in Figure 1.7. Recently, EC-SPR spectroscopy has been used to study the electrical and optical characteristics of conductive polymer substrate. Therefore, CPs such as PEDOT/PSS, polypyrrole and P2ABA also show impressive performance and potential, which can be combined with various optical technologies to make effective sensors and biosensors [28].

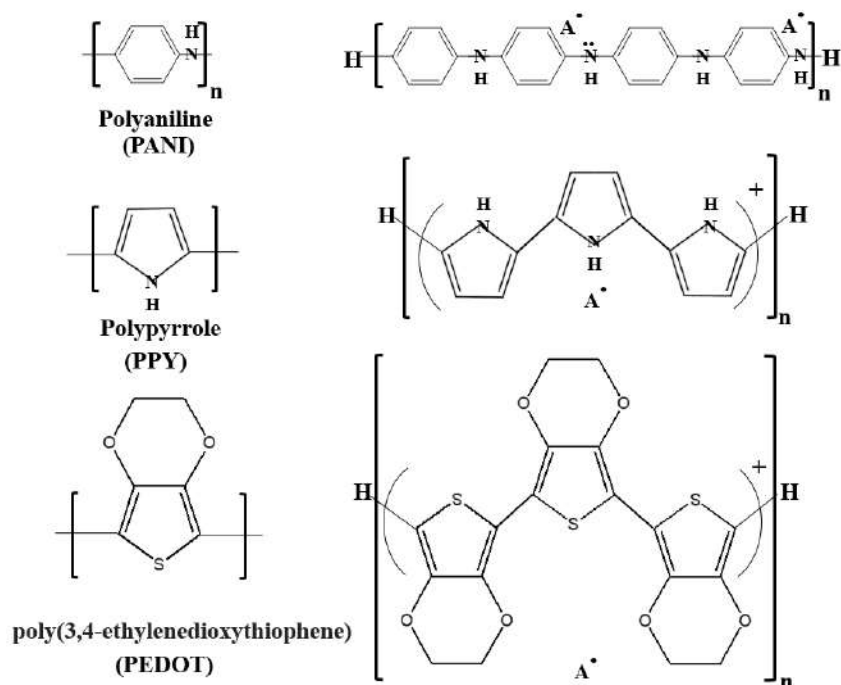


Figure 1.7 Chemical structures of the various conducting polymers.

### **1.5.2 GRAPHENE OXIDE BASED SPR BIOSENSORS**

Graphene oxide (GO) contains a carbon sheet based on a hexagonal ring, the carbon sheet contains one  $sp^2$  hybridized carbon atom and one  $sp^3$  hybridized carbon atom, with an epoxide functional group and hydroxyl group on each side of the sheet. The edge plane is primarily decorated by carbonyl and carboxyl bunches [29]. These properties of GO are promising for many applications such as nano-electronics, nanocomposites, nanophotonics, and biosensors [30]. SPR is another interesting research area to expand the application of GO. GO can provide new insights for SPR behavior: (1) as a tunable excitation and propagation surface, its optical properties can be adjusted by exterior electromagnetic fields, (2) as a surface that directly supports surface plasmons in the range of visible light, and (3) as an oxygen functional group covering existing plasma devices. This oxygenic-containing functional group in graphene oxide presents the bandgap energy and an option to adjust the electronic, mechanical, and optical properties [31].

### **1.5.3 METAL NANOPARTICLES**

The optical properties of silver (Ag) and gold (Au) nanoparticles have established a lot of consideration due to their potential in biochemical and chemical measurements medical diagnostics/therapeutics, and biological imaging [32]. The resonance coupling of the combined oscillation mode of the incident light and the conduction electrons in the noble metal nanoparticles has the function of optimizing the generally observed improvement in light absorption. It can also be accompanied by strong diffusion as a minor process, typically when the particle size is greater than 10 nanometers. The size of the scattering efficiency and

the relative influence on overall extinction are shown to vary with the size and shape of the particles, the metallic element, and the surrounding medium [33]. Optical scattering can be used to detect the imaging method of connected biological systems. In sensor applications, the change in the maximum absorption or dispersion of the plasmon resonance wavelength as a act of changes in the physical and chemical environment of the nanoparticle surface is studied [34]. Therefore, a high sensitivity of the spectral signal of the plasmon resonance absorption or scattering band is required to variations in the refractive index of the medium.

## **1.6 BIOMARKERS**

### **1.6.1 IMMUNOGLOBULIN G (IgG)**

IgG is a plasma cell protein produced in the bone marrow, lymph nodes, spleen, small intestine mucosa, thymus, respiratory tract mucosa, and other tissues [35]. Since IgG is produced as part of the body's response to bacteria, drugs, viruses, and tissue antigens, the measurement of IgG levels in the blood may reveal hypersensitivity to antigen stimulation or physiological abnormalities in the IgG production site, as well as other diseases. Therefore, human IgG levels are often measured in immunological and allergic reaction tests [36].

### **1.6.2 CREATININE**

Creatinine is the end product of creatinine metabolism and is eliminated by the renal system at a constant rate. Changes in blood and urine creatinine levels reflect some abnormalities, such as urinary tract obstruction, kidney disease, muscular dystrophy, and muscle weakness. Creatinine levels is a reliable clinical biomarker for monitoring these complications [37].

## **1.7 CHARACTERIZATION TECHNIQUES**

### **1.7.1 ATOMIC FORCE MICROSCOPY**

Atomic force microscopy (AFM) is a technique of imaging the surface of any type of material, such as glass, polymers, composites, biological samples, and ceramics. AFM is used to measure and locate numerous different forces, including magnetic force, adhesion, and mechanical properties. The AFM consists of a sharp tip with a diameter of approximately 10-20 nm, which is attached to the overhang. Therefore, AFM characterization provides an attractive and non-destructive method of inspecting surface properties [38].

### **1.7.2 UV-VIS SPECTROSCOPY**

The basic principles of organic molecules absorbing, emitting and scattering UV-Vis light can be described by the Jablonski diagram (Figure 1.5). The horizontal line represents the grounded singlet state and excited state, the excited state electronic triplet state, and the short-term simulated energy level that exists during the interaction. scattering. Each electronic singlet and triplet state is divided into sub-levels of vibration and rotation energy [39].

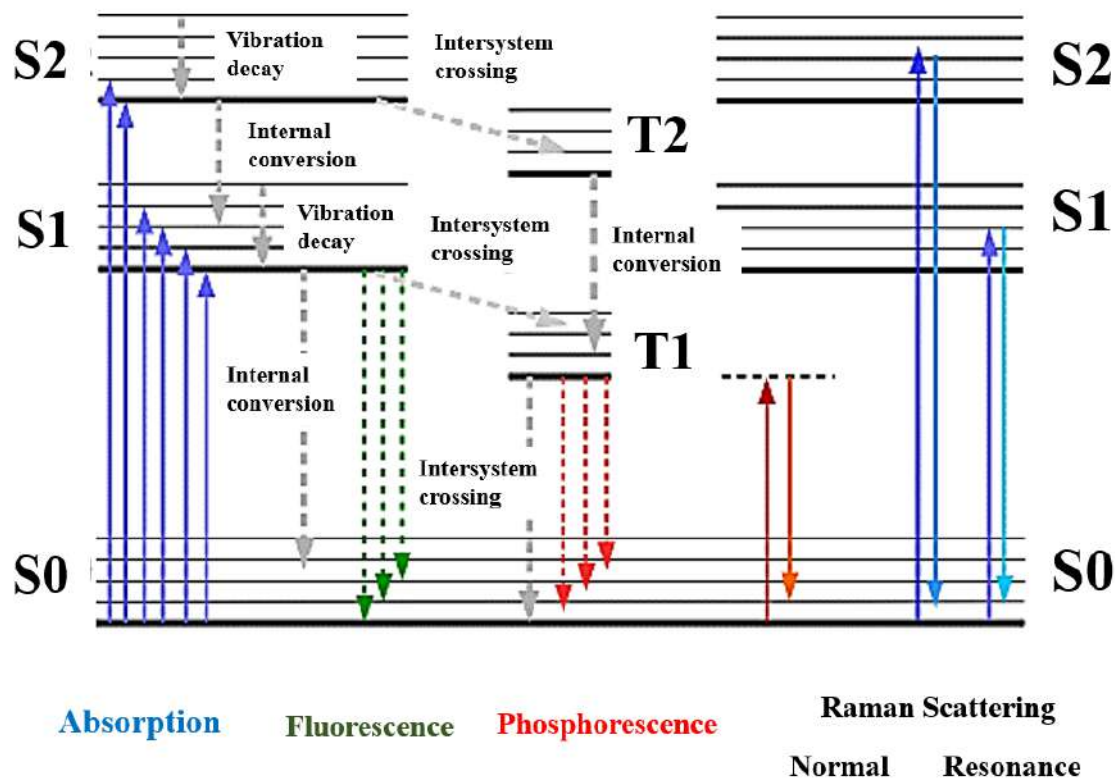


Figure 1.8 Jablonski-type energy level diagram, showing the absorption, emission, and scattering of UV-Vis light, and non-radiative transitions.

### 1.7.3 IMAGING TECHNOLOGY

Due to the growing demand for mobile imaging, digital cameras and camcorders, Internet-based video conferencing, surveillance, and biometric technology, the solid-state imaging sensor market has seen explosive development in recent years. Image sensors have become a major driving force for silicon technology. Charge coupled devices (CCDs) are regularly the main image sensor technique. The latest developments in the construct of image sensors employed in complementary metal oxide semiconductor (CMOS) technology have

led to its adoption in a variety of high-volume products, such as mobile phones, optical mice, PC cameras, and cameras high-end digital devices. Additionally, by leveraging the ability to integrate detection with pixel-level digital and analog processing, new CMOS imaging devices are being created for applications such as machine interface, machine vision, survey and monitoring, and biological testing [40].

## **1.8 OBJECTIVES**

1. To prepare and construct the functional nanomaterials and EC-SPR sensing platforms, respectively.
2. To study in situ EC-SPR biosensors for the detection of biomarkers.
3. To study device performances with the optimization, kinetic study, and electrochemical control.
4. To study T-SPR biosensors for the detection of biomarkers.
5. To study TSPR-image biosensors for the detection of biomarkers.

## **1.9 SCOPE OF THESIS**

Biosensors based on the SPR technique combined with the characteristic specificity of the recognition elements on our fabricated electrochemical transducers, allowing selective and sensitive detection of the analytes without labeling will be demonstrated in this work. Our goal in chapter 2 is to develop SPR and electrochemical techniques combined with SPR spectroscopy to generate a novel and effective molecular recognition technology for enhancing analytical signal. The SPR and EC-SPR platforms based on functionalized

conducting polymer nanocomposites will be synthesized using electrochemical techniques and biofunctionality will be constructed and studied. The structural and optical properties of the conducting polymer nanocomposite film on gold support will be characterized using EC-SPR measurements. SPR signal with the EC control experiments will be studied in order to obtain highest sensitivity in the detections of IgG biomarkers. The interaction of biomolecules on the bioplayers will be studied. In chapter 3 our goal was to investigate TSPR and TSPR-imaging of thin film-based biosensor application. In chapter 4 our purpose was to prepare silver nanoparticles on a PPy thin film based SPR for detection of creatinine sensor.

Furthermore, the SPR, EC-SPR and TSPR platforms will be characterized using many potential techniques such as UV-visible, AFM, SPR spectroscopies, and electrochemical methods. In terms of sensing applications, the platforms will be used as electrochemical SPR biosensors for detections of biomarkers. The conditions for detection and device fabrication will be optimized and will be applied to the detection in clinical samples. Therefore, three work chapters are included as follows:

1. SPR and EC-SPR immunosensor for detection of human immunoglobulin G
2. Development of TSPR and TSPR-imaging-based biosensor for detection of IgG
3. Development of SPR-based AgNPs/PPy thin film for detection of creatinine

## 1.10 REFERENCES

- [1] S.F. Kingsmore, Multiplexed protein measurement: technologies and applications of protein and antibody arrays, *Nature Reviews Drug Discovery*, 5(2006) 310-320.
- [2] V. Perumal, U. Hashim, *Advances in biosensors: Principle, architecture and applications*, *Journal of Applied Biomedicine*, 12(2014) 1-15.
- [3] M.S. Thakur, K.V. Ragavan, *Biosensors in food processing*, *Journal of Food Science and Technology*, 50(2013) 625-641.
- [4] A. Hasan, M. Nurunnabi, M. Morshed, A. Paul, A. Polini, T. Kuila, et al., *Recent advances in application of biosensors in tissue engineering*, *BioMed research international*, 2014(2014) 307519.
- [5] E. Helmerhorst, D.J. Chandler, M. Nussio, C.D. Mamotte, *Real-time and label-free biosensing of molecular interactions by surface plasmon resonance: A laboratory medicine perspective*, *The Clinical Biochemist Reviews*, 33(2012) 161-73.
- [6] W. Wang, Z. Mai, Y. Chen, J. Wang, L. Li, Q. Su, *A label-free fiber optic SPR biosensor for specific detection of C-reactive protein*, *Scientific Reports*, 7(2017) 16904.
- [7] D. Grieshaber, R. MacKenzie, J. Vörös, E. Reimhult, *Electrochemical biosensors - sensor principles and architectures*, *Sensors*, 8(2008) 1400-1458.
- [8] P. Damborský, J. Švitel, J. Katrlík, *Optical biosensors*, *Essays Biochem*, 60(2016) 91-100.
- [9] I.I. Ebralidze, N.O. Laschuk, J. Poisson, O.V. Zenkina, *Chapter 1 - Colorimetric Sensors and Sensor Arrays*, in: O.V. Zenkina (Ed.) *Nanomaterials Design for Sensing Applications*, Elsevier2019, 1-39.



- [10] B. Mondal, S. Ramlal, P.S. Lavu, B. N, J. Kingston, Highly sensitive colorimetric biosensor for staphylococcal enterotoxin B by a label-free aptamer and gold nanoparticles, *Frontiers in Microbiology*, 9(2018).
- [11] V.X.T. Zhao, T.I. Wong, X.T. Zheng, Y.N. Tan, X. Zhou, Colorimetric biosensors for point-of-care virus detections, *Materials Science for Energy Technologies*, 3(2020) 237-49.
- [12] S. Mariani, M. Minunni, Surface plasmon resonance applications in clinical analysis, *Analytical and bioanalytical chemistry*, 406(2014) 2303-2323.
- [13] F.B. Kamal Eddin, Y.W. Fen, The principle of nanomaterials based surface plasmon resonance biosensors and its potential for dopamine detection, *Molecules*, 25(2020) 2769.
- [14] Y. Yanase, T. Hiragun, K. Ishii, T. Kawaguchi, T. Yanase, M. Kawai, Surface plasmon resonance for cell-based clinical diagnosis, *Sensors*, 14(2014) 4948-4959.
- [15] R. Peltomaa, B. Glahn-Martínez, E. Benito-Peña, M.C. Moreno-Bondi, Optical biosensors for label-free detection of small molecules, *Sensors*, 18(2018) 4126.
- [16] D.M. Kim, J.S. Park, S.-W. Jung, J. Yeom, S.M. Yoo, Biosensing applications using nanostructure-based localized surface plasmon resonance sensors, *Sensors*, 21(2021).
- [17] M. Li, S.K. Cushing, N. Wu, Plasmon-enhanced optical sensors: a review, *Analyst*, 140(2015) 386-406.
- [18] S. Szunerits, R. Boukherroub, Sensing using localised surface plasmon resonance sensors, *Chemical Communications*, 48(2012) 8999-9010.
- [19] F.-C. Lin, K.-M. See, L. Ouyang, Y.-X. Huang, Y.-J. Chen, J. Popp, Designable spectrometer-free index sensing using plasmonic doppler gratings, *Analytical Chemistry*, 91(2019) 9382-9387.

- [20] B.K. Singh, A.C. Hillier, Surface plasmon resonance enhanced transmission of light through gold-coated diffraction gratings, *Analytical Chemistry*, 80(2008) 3803-3810.
- [21] J. Golden, M.D. Yates, M. Halsted, L. Tender, Application of electrochemical surface plasmon resonance (ESPR) to the study of electroactive microbial biofilms, *Physical Chemistry Chemical Physics*, 20(2018) 25648-25656.
- [22] J. Juan-Colás, S. Johnson, T.F. Krauss, Dual-mode electro-optical techniques for biosensing applications: A Review, *Sensors*, 17(2017) 2047.
- [23] S. Ramanavicius, A. Ramanavicius, Conducting polymers in the design of biosensors and biofuel cells, *Polymers*, 13(2020) 49.
- [24] F. Wei, S. Cheng, Y. Korin, E.F. Reed, D. Gjertson, C.-m. Ho, Serum creatinine detection by a conducting-polymer-based electrochemical sensor to identify allograft dysfunction, *Analytical chemistry*, 84(2012) 7933-7937.
- [25] G.B. Tseghai, D.A. Mengistie, B. Malengier, K.A. Fante, L. Van Langenhove, PEDOT:PSS-based conductive textiles and their applications, *Sensors*, 20(2020).
- [26] R. Janmanee, S. Chuekachang, S. Sriwichai, A. Baba, S. Phanichphant, Functional conducting polymers in the application of SPR biosensors, *Journal of Nanotechnology*, 2012(2012) 620309.
- [27] S. Chuekachang, R. Janmanee, A. Baba, S. Phanichphant, S. Sriwichai, K. Shinbo, Fabrication of thin film from conducting polymer/single wall carbon nanotube composites for the detection of uric acid, *Molecular Crystals and Liquid Crystals*, 580(2013) 1-6.

- [28] N.S. Ramdzan, Y.W. Fen, N.A. Anas, N.A. Omar, S. Saleviter, Development of biopolymer and conducting polymer-based optical sensors for heavy metal ion detection, *Molecules*, 25(2020).
- [29] W. Yu, L. Sisi, Y. Haiyan, L. Jie, Progress in the functional modification of graphene/graphene oxide: a review, *RSC Advances*, 10(2020) 15328-15345.
- [30] N.-F. Chiu, C.-C. Chen, C.-D. Yang, Y.-S. Kao, W.-R. Wu, Enhanced plasmonic biosensors of hybrid gold nanoparticle-graphene oxide-based label-free immunoassay, *Nanoscale Research Letters*, 13(2018) 152.
- [31] Y. Li, Z. Li, C. Chi, H. Shan, L. Zheng, Z. Fang, Plasmonics of 2D nanomaterials: properties and applications, *Advanced Science*, 4(2017) 1600430.
- [32] K.-S. Lee, M.A. El-Sayed, Gold and silver nanoparticles in sensing and imaging: sensitivity of plasmon response to size, shape, and metal composition, *The Journal of Physical Chemistry B*, 110(2006) 19220-19225.
- [33] X. Huang, M.A. El-Sayed, Gold nanoparticles: Optical properties and implementations in cancer diagnosis and photothermal therapy, *Journal of Advanced Research*, 1(2010) 13-28.
- [34] M. Li, S.K. Cushing, N. Wu, Plasmon-enhanced optical sensors: a review, *The Analyst*, 140(2015) 386-406.
- [35] E.J. Kunkel, E.C. Butcher, Plasma-cell homing, *Nature Reviews Immunology*, 3(2003) 822-9.
- [36] X. Wang, G.-L. Hao, B.-Y. Wang, C.-C. Gao, Y.-X. Wang, L.-S. Li, et al., Function and dysfunction of plasma cells in intestine, *Cell Bioscience*, 9(2019) 26.

- [37] A. Arif Topçu, E. Özgür, F. Yılmaz, N. Bereli, A. Denizli, Real time monitoring and label free creatinine detection with artificial receptors, *Materials Science and Engineering: B*, 244(2019) 6-11.
- [38] W. Fu, W. Zhang, Hybrid AFM for nanoscale physicochemical characterization: recent development and emerging applications, *Small*, 13(2017) 1603525.
- [39] J.M. Antosiewicz, D. Shugar, UV–Vis spectroscopy of tyrosine side-groups in studies of protein structure. Part 1: basic principles and properties of tyrosine chromophore, *Biophysical Reviews*, 8(2016) 151-161.
- [40] A.E. Gamal, H. Eltoukhy, CMOS image sensors, *IEEE Circuits and Devices Magazine*, 21(2005) 6-20.

## **CHAPTER 2**

### **SURFACE PLASMON RESONANCE BASED BIOSENSORS FOR DETECTION OF HUMAN IMMUNOGLOBULIN G**

#### **2.1 INTRODUCTION**

The most abundant antibody in the human body is IgG [1]. Diseases like systemic lupus erythematosus and hyperthyroidism occur when the IgG concentration is greater or lower than normal level. Therefore, the detection of human IgG level is very important in the fields of medical diagnosis, drug research and quality control [2]. SPR-based biosensors have been researched in recent years. They are broadly utilized for many essential industrial and medical fields, for example, the immunoreaction of antigen-antibody monitoring, food safety detection, and environmental checking [3]. By monitoring the refractive index change of the near-surface reagent, the SPR biosensor can offer real-time, reproducible, and sensitive detection for target analysis. The fabrication of a fiber optic SPR sensor needs the use of a rotating vacuum sputtering or evaporation process to confirm that the gold film is deposited uniformly on the fiber optic sensor's surface. The effective techniques of immobilizing functional molecules are still needed to generate more capturing sites for target molecules and improve SPR sensitivity analyses [4]. A thin film of metal coating is placed to the sensor's surface for fiber optic SPR sensors. Gold film is popular because it resists oxidation and corrosion in a variety of circumstances [5]. However, the effect of immobilized biomolecules is unproductive, and the number of molecules absorbed is insufficient if only the thiol groups

are founded, which limits the development of gold film for biosensors. Furthermore, the gold-coated SPR sensor needs the use of complicated and expensive rotary vacuum evaporation or sputtering processes [6]. Chemical approaches have gained a lot of interest in the manufacturing of SPR sensors as an alternative to using metal thin film coatings. The chemical approach, unlike sputtering, requires low-cost or complicated equipment, and the thickness and character of the coating film may be controlled by adjusting the reagent concentration and reaction time. The SPR sensor made of conductive polymer film features a strong resonance peak and excellent detection accuracy [7]. However, the polymer is unstable. Therefore, other nanomaterials have been applied for the combination with polymer to improve the stability of the sensor. GO has been frequently employed in SPR sensors in recent years. GO is a carbon allotrope with one atom at each vertex in a two-dimensional structure, and atomic-level hexagonal pattern [8]. Due to GO has simple for modification and a great specific surface area of atomic monolayer, it can be used to detect gases, humidity, and temperature [9]. Furthermore, as compared to graphene, GO has superior properties such as high solubility, good biocompatibility, and high selectivity. GO-enriched functional groups can interact ionically, covalently, or non-covalently, GO has the best biomolecule extraction efficiency per unit area [10]. The reagents that are fixed on the metal film at the surface or on a component of the sensor are also crucial to the SPR biosensor's performance. By connecting the amine group to the activated carboxyl surface with N-hydroxysulfosuccinimide (NHS) and 1-ethyl-3-(3-(dimethylamino)propyl)-carbodiimide hydrochloride (EDC), antibody fixing efficiency is improved. In Section 2.3, the GO/poly(2-aminobenzylamine)-based SPR for IgG detection is discussed.

Electrochemical surface plasmon resonance has been incorporated to these combined EC-SPR. SPR is the foundation of EC-SPR. SPR is an optical technology that is extremely sensitive to refractive index changes. Changes in composition at the interface between the aqueous solution and the conductive surface cause changes in the refractive index. SPR is commonly used to investigate adsorption and other molecular interactions, such as antibody-antigen binding, in which one (antibody or antigen) is immobilized on the surface and the other is coupled to it [11, 12]. The conductive surface serves as a working electrode in EC-SPR, allowing optical control of electrochemical processes via changes in the interface refractive index caused by changes in the oxidation state of redox molecules at the electrode surface [13].

In Section 2.4, the SPR membrane substrate is first produced by GO electrolysis and monomer solution to generate the EC-SPCE immunosensor. The morphology of the polymer is altered when an applied potential allows antibodies immobilized on GO to display on the surface of the film/electrolyte interface. The sensitivity is thus improved due to the high number of captured antigens, human IgG and the suitable identification of antibodies with better detection.

## **2.2 EXPERIMENTAL DETAILS**

### **2.2.1 CHEMICALS AND MATERIALS**

2-Aminobenzylamine (2ABA) was obtained and used from Tokyo Kasei Kogyo Co, Ltd (Japan). GO powder was synthesized using the modified Hummer's method. Phosphate buffered saline (10 mM PBS, pH 7.4), immunoglobulin G (Anti-IgG), immunoglobulin G (human IgG), ethanolamine hydrochloride (EA-HCl) tablets 3,4-ethylenedioxythiophene (EDOT), and poly(4-styrene sulfonate) (PSS), were obtained by Sigma Aldrich USA). 1-Ethyl-3-(3-dimethylaminopropyl) carbodiimide hydrochloride (EDC) and N-hydroxysuccinimide (NHS) were obtained from Tokyo Chemical Industry and Wako Pure Chemical Industries (Japan), respectively. Deionized (DI) water (18 M $\Omega$ , Eyela Still Ace SA-2100E1) was used to make all aqueous solutions.

### **2.2.2 EC-SPR INSTRUMENTATION**

A research laboratory-developed lessened total reflection (ATR) structure with a typical Kretschmann design and 3 electrochemical cell was used to evaluate SPR reflectivity. A He-Ne laser with a wavelength of 632.8 nm was used as the excitation source. A gold-coated high-refractive index glass electrode was made using vacuum evaporation of chromium and gold with the thickness of 3 nm and 47 nm, respectively. For future polymerization, immobilization, electrochemical, and sensing tests, the gold film was constructed. For electropolymerization and electrochemical investigation, the gold SPR substrate was employed as the working electrode (surface area 0.635 cm<sup>2</sup>), Ag/AgCl



reference electrode (in 3M NaCl), and Pt wire electrode. A potentiostat (HZ-5000 potentiostat, Hokuto Denko Ltd., Japan) was used to record the CV measurement.

## **2.3 A GRAPHENE OXIDE/POLY(2-AMINOBENZYLAMINE)-BASED SURFACE PLASMON RESONANCE IMMUNOSENSORS**

### **2.3.1 CONSTRUCTION OF GO/P2ABA/GOLD-BASED IMMUNOSENSOR**

GO/P2ABA was electrodeposited on a gold-coated high reflective glass. Au/GO/P2ABA surface was washed with DI water 3 times. To activate the carboxylic groups on the surface, a mixed solution of 0.4 M EDC and 0.1 M NHS at a volume ratio of 1: 1 is employed. Anti-IgG was immobilized on the surface after washing with DI water. The solution was then washed with PBS buffer before being injected into Teflon cells with 0.2 M EA-HCl solution to prevent nonspecific binding. The solution was then washed with PBS buffer for 5 minutes. Human IgG molecules were functionalized on the activated surface in various concentrations. The SPR sensor's response was seen on the immobilized IgG surface by assessing the intensity change. The SPR setup diagram and step of the SPR immunosensor for IgG detection are presented in Figure 2.1.

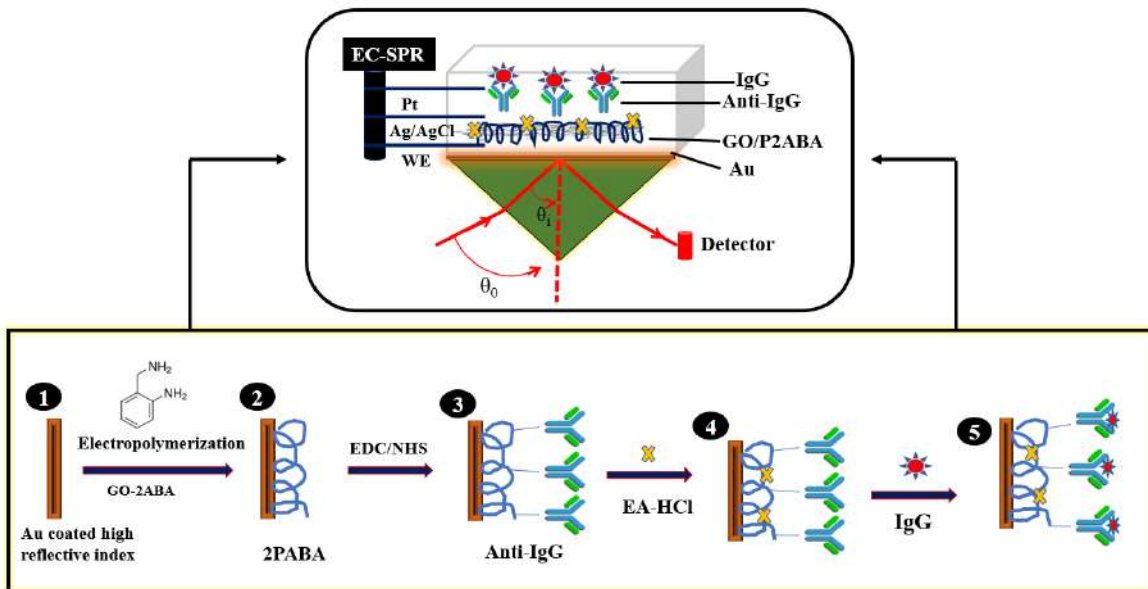


Figure 2.1 SPR setup and step of SPR immunosensor for IgG detection.

### 2.3.2 RESULTS AND DISCUSSION

The CV curve of the electrochemical polymerization of 2ABA to form P2ABA is shown in Figure 2.2 (a). The CVs curve of the electrochemical polymerization of GO/2ABA to form the GO/P2ABA composite on the gold electrode is shown in Figure 2(b). According to the CV curves, the anode current over 0.60 V improved with the number of polymerization cycles, implying the creation of a P2ABA polymer on a gold surface. The number of electropolymerization cycles increased the redox current between 0.6 and -0.5 V, indicating film deposition. In the similar cycle, the anodic peak current with GO is increased at 1.1 V when compared to electropolymerization without GO (highest oxidation potential). According to the CV curve in figure 2.2 (c), the current of the GO/P2ABA/gold substrate is

greater than the current of the P2ABA/gold film. This is most likely due to the fact that the thickness of GO/P2ABA is slightly bigger than that of P2ABA.

SPR reflectivity curves of only gold, P2ABA/gold, and GO/P2ABA/gold electrodes are shown in Figure 2.2 (d). The angle of the SPR increased after the electropolymerization procedure, suggesting that the P2ABA and GO/P2ABA films had formed on the gold electrode and that the reflection intensity of the two films at the angle of inclination is greater than the bare gold. The SPR angle of the GO/P2ABA electrode is bigger than that of the P2ABA film. In addition, the SPR kinetics of IgG are investigated using P2ABA and GO/P2ABA films on gold electrodes. Figure 2.2 (dashed line) (e). shows the improvement in IgG detection in GO/P2ABA (solid line) as compared to P2ABA.

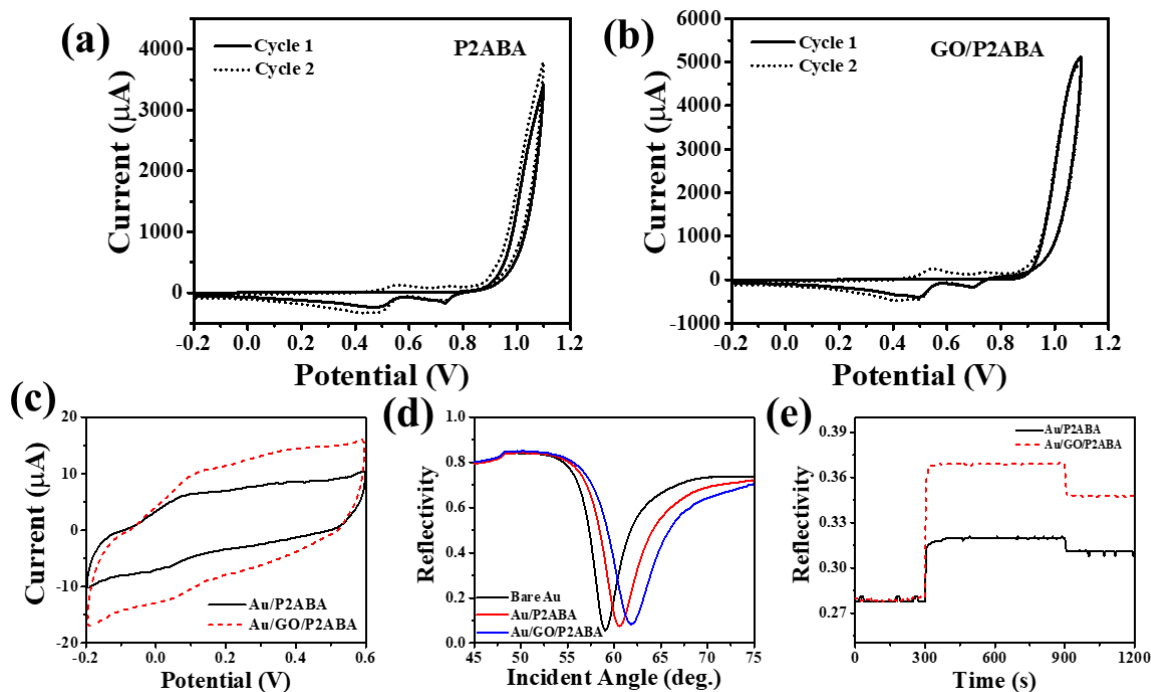


Figure 2.2 (a) CV curve for 2 cycles of electropolymerization of P2ABA (b) CV curve for electropolymerization of GO/P2ABA for 2 cycles (c) CV curve of P2ABA and GO/ P2ABA in gold film in solution of PBS (d) SPR angular reflectivity curve of gold substrate, P2ABA/gold, and GO/P2ABA/gold (e) SPR kinetics of P2ABA/gold and GO/P2ABA/gold, used to detect 10 μg/ml of IgG.

For the subsequent construction of the immunosensor, the electrode of the obtained GO/P2ABA membrane is investigated in PBS solution at pH 7.4. The potential from -0.2 to 0.6 V in a scan rate varying from 20 to 100 mV/s. The results suggest that the GO/P2ABA film is electroactive in this neutral solution, as illustrated in Figure 2.3 (a). In addition, the corresponding graph of the anodic and cathode peak currents versus rotational speed is shown in Figure 2.3 (b). Observation of the histogram indicates that the GO/P2ABA oxidation

exhibits good linearity with respect to the increase in scan rates. The results of the linear relationship between  $I_{pa}/I_{pc}$  and the scan rate indicate that the GO/P2ABA oxidation and reduction is a controlled surface process.

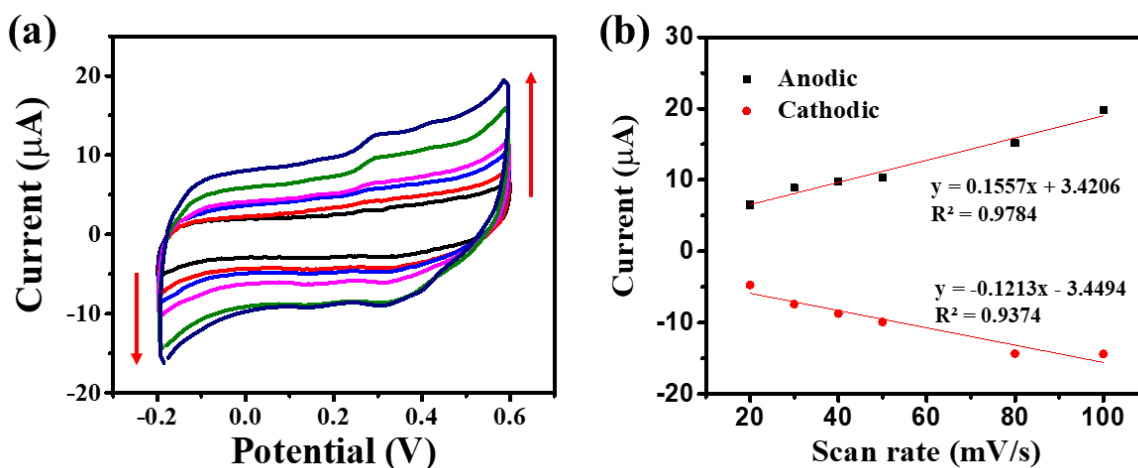


Figure 2.3 (a) CV curves of Au/GO/P2ABA film at several scan rates from 20 to 100 mV/s in PBS solution (b) and the plots of anodic and cathodic peak current with scan rate.

Anti-human IgG immobilization on the surface of GO/P2ABA and anti-human IgG binding to human IgG are monitored in real time using the SPR method. The simultaneous SPR kinetic graph in the construction of the GO/P2ABA-based immune response is shown in Figure 2.4. The intensity of the SPR response increases because of the surface modification process. The SPR baseline was initially obtained using a PBS solution with a pH of 7.4. The COOH groups and amine groups are introduced into the substrate by the deposited GO/P2ABA film, which can then be activated for anti-IgG immobilization. To activate the COOH groups on the surface, we injected a 1: 1 solution mixture EDC/NHS as a coupling agent for 5 minutes to promote covalent bonding on the surface of the GO/P2ABA film

making NHS ester. During the activation process, the SPR intensity increases, suggesting that the carboxyl group has been activated and a stable chemical intermediate has formed. After washing with PBS solution, the SPR intensity decreased and became stable. The intensity of the SPR was enhanced again after injecting a 100  $\mu\text{g/mL}$  anti-human IgG solution to acquire the amide bond between the anti-human IgG and the activated surface. The intensity of the SPR gradually increased after 5 minutes of rinsing with PBS solution and 5 minutes of treat with EA-HCl solution, showing that the remaining free binding sites are inactive. After washing with PBS solution and injecting human IgG, the SPR response increased, showing that anti-human IgG attach with human IgG. Finally, after injection of the PBS solution, the SPR signal reduced and remained steady due to some dissociation of IgG.

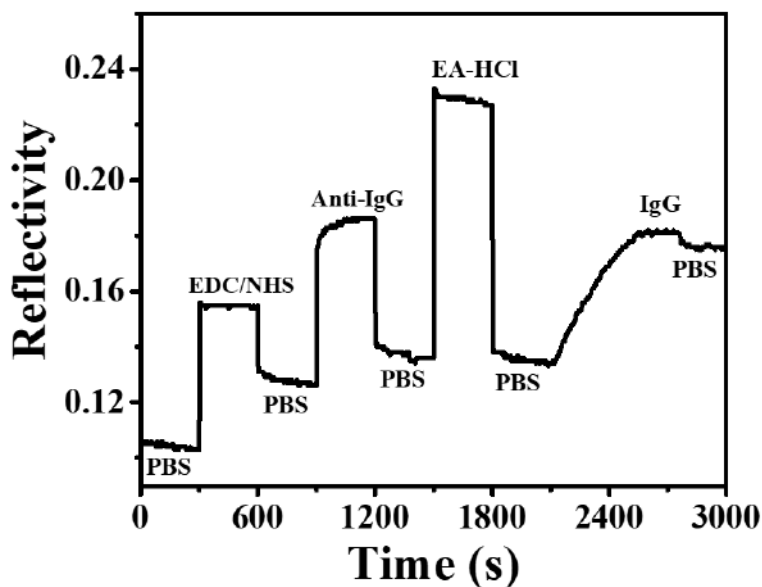


Figure 2.4 SPR response to detect human IgG (10  $\mu\text{g/mL}$ ) through the creation of Au/GO/P2ABA-based immunosensor.

The GO/P2ABA-based immunosensor is compared to the P2ABA-based immunosensor in terms of sensitivity. Figure 2.4 shows the SPR responses for detecting human IgG on anti-human IgG/GO/P2ABA films with the anti-human IgG/P2ABA system. The sensitivity of the relationship between SPR intensity change and human IgG levels on GO/P2ABA film is higher than that of the P2ABA-based IgG immunosensor. To determine the LOD of the assay, IgG antibodies are reacted with IgG immobilized on the surface of the sensor. When the IgG concentration is decreased from 1.0 to 10 M, a proportional change in the SPR response is observed (Figures 2.5(a)) and (b)) indicating an efficient interaction between the IgG and IgG antibodies. The change in SPR intensity caused by specific recognition of IgG and anti-IgG is displayed of immobilized IgG with difference concentration in Figure 2.5 (c). When anti-IgG/GO/P2ABA/Au is used to detect IgG, the sensitivity is 1.4 times higher than when no GO is used. These findings suggest that GO can improve the sensitivity of the SPR immunosensor's detection of IgG concentration.

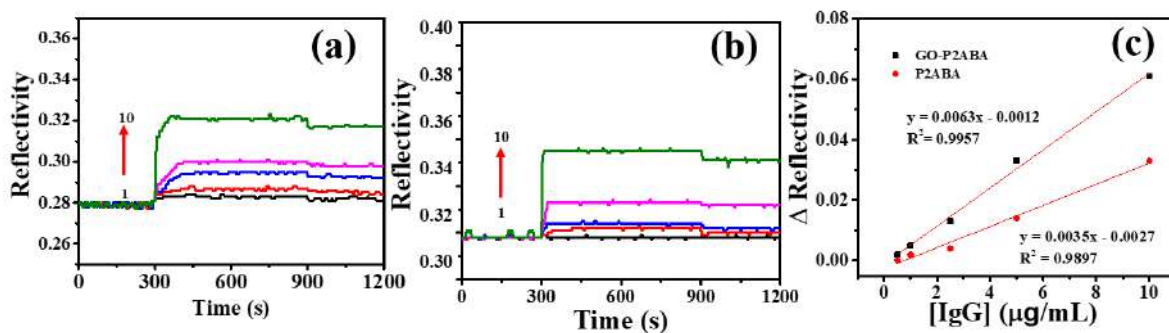


Figure 2.5 SPR kinetics as a function of IgG concentration. (a) P2ABA, (b) GO / P2ABA and (c) two calibration curves for the detection of IgG and GO.

### 2.3.3 CONCLUSION

We present an optical SPR immunosensor with a good sensitivity and low LOD for detection of human IgG that has been modified by an anti-human IgG/P2ABA/GO film. Ionic, covalent, and non-covalent interactions between GO-rich functional groups can increase the change in resonance wavelength. The P2ABA/GO detection surface is then further functionalized for anti-human IgG, allowing it to detect human IgG at various concentrations in the range from 1.0 to 10  $\mu\text{g/mL}$  with a LOD as 0.95  $\mu\text{g/mL}$ . The results established the possibility of the proposed biosensor. Furthermore, the suggested P2ABA/GO biosensor functions as a bioanalysis platform for real-time monitoring, label-free, and numerous in clinical applications.



## **2.4 ELECTROCHEMICAL SURFACE PLASMON RESONANCE IMMUNOSENSOR-BASED GRAPHENE OXIDE/POLY(3,4 ETHYLENEDIOXYTHIOPHENE)/ POLY(STYRENE SULFONATE) THIN FILM**

### **2.4.1 FABRICATION OF GO/PEDOT/PSS ELECTRODE**

The mixtures solution including 1.0 mg/mL GO, 0.10 % v/v EDOT, and 0.70 % w/v PSS solution were dispersed under sonication for 30 minutes. The mixture solution (GO-EDOT-PSS solution) were electropolymerized on the gold-coated high refractive index glass electrode by an applied potential range from 0.0 to 0.90 V at a scan rate of 20 mV/s for 5 cycles (no mixture of GO for the PEDOT/ PSS substrate).

### **2.4.2 PREPARATION OF EC-SPR BIOSENSOR**

The GO/PEDOT/PSS electrode was utilized in the electrochemical control testing and the immunosensor was developed by covalently functionalizing anti-IgG and then detecting IgG. Anti-IgG was covalently attached to the film by the -COOH groups of GO via an amide coupling process. EDC/NHS solution was added for 5 minutes to activation of the -COOH group in the GO structure, subsequently washed three times with PBS buffer. After that, 100 µg/mL anti-IgG solution was used to immobilize the protein for 5 minutes. The electrode was incubated in 0.20 M EA-HCl solution to prevent non-specific binding sites and keep on active sites at the surface of electrode. The GO/PEDOT/PSS biosensor was utilized to assay human IgG with the different concentrations from 1.0 to 10 µg/mL. 1.0 mg/mL GO was

utilized for detection of human IgG. To optimize electrochemical control, constant potentials at -1.0, -0.65, -0.2, 0.50 and 1.0 V were applied in 10 mM PBS solution at pH 7.4 and the open circuit (without applied potential) of the biosensor-based GO/PEDOT/PSS was also investigated. The sensitivity and LOD might be changed by employing different constant potentials. The maximum sensitivity would be related to the electrochemical control of the correct location of the GO/PEDOT/PSS electrode. Figure 2.6 depicts a schematic illustration of the prepared GO/PEDOT/PSS-based biosensor for the assay of IgG.

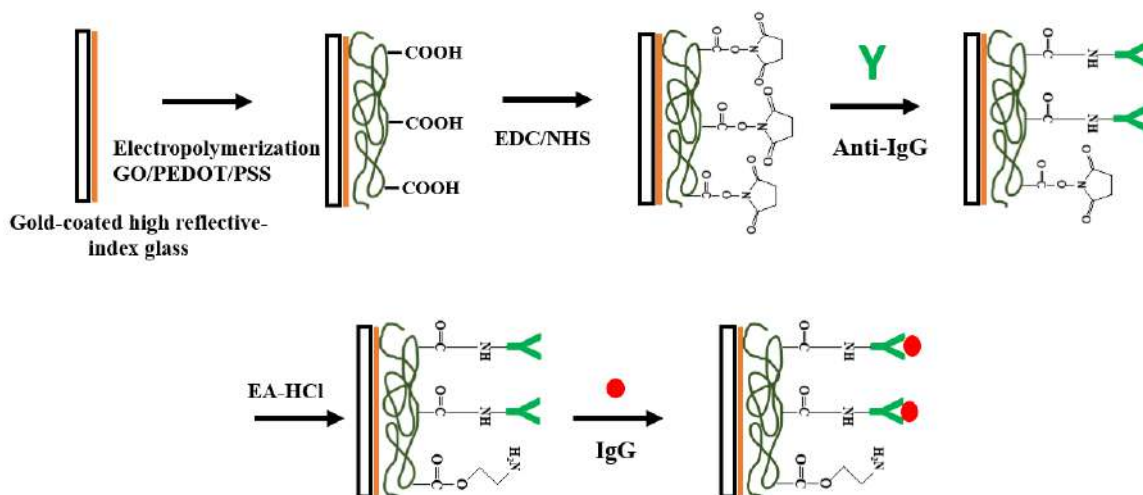


Figure 2.6 Schematic illustration of a GO/PEDOT/PSS-based biosensor for recognition of IgG.

## **2.4.3 RESULTS AND DISCUSSION**

### **2.4.3.1 FRABRICATION AND DESCRIPTION OF GO/PEDOT/PSS**

#### **FILM**

The -COOH group in GO structure is introduced of the GO/PEDOT/PSS at the electrode surface, which is easily swelled and dispersed in water and has a good hydrophilicity. GO is utilized as a co-dopant with PSS solution during the electropolymerization of the GO/PEDOT/PSS electrode. The CV responses for the electrodeposition of PEDOT/PSS and GO/PEDOT/PSS films on Au electrodes are shown in Figures 2.7 (a) and 2.7 (b). The electropolymerization is carried out for 5 cycles in the scan rate of 20 mV/s with the dispersion solution containing GO, EDOT monomer, and PSS solution (without GO added for PEDOT/PSS deposition). The anodic current over 0.70 V increased with the amount of electrodeposition cycles, demonstrating the creation of the polymer structure on gold electrode, according to the CV curves.

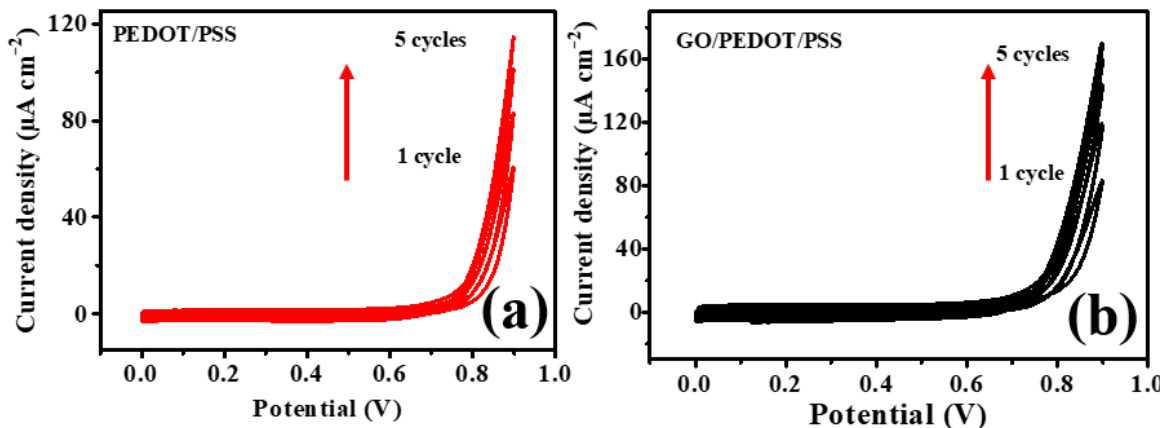


Figure 2.7 Electropolymerization curves for (a) PEDOT/PSS, (b) GO/PEDOT/PSS, and (c) gold coated SPR chip films.

Figure 2.8 (a) illustrates the SPR reflectivity curves for only gold, PEDOT/PSS, and GO/PEDOT/PSS substrates. The SPR reflectivity improved after electrodeposition, signifying the structure of PEDOT/PSS and GO/PEDOT/PSS layers on the Au electrode, with SPR curves of both layers at dip angles greater than the bare substrate. The GO/PEDOT/PSS thin film's SPR substrate dip angle changed to a higher amount than that of the PEDOT/PSS electrode. These findings show that during electropolymerization, GO could be added in the PEDOT structure as a dopant at the same time with the polyanion from PSS structure. The redox signal of the GO/PEDOT/PSS structure is greater than that of the PEDOT/PSS structure, as seen by the CV curve in Figure 2.8 (b). It might be because GO/PEDOT/PSS is a little thicker than PEDOT/PSS. Another possibility is that the integration of GO into the PEDOT/PSS structure improves relative surface area and electroactivity. Figure 2.8 (c) shows SPR reflectivity curves obtained at various constant potentials to investigate the optical characteristics of doped and de-doped GO/PEDOT/PSS

layers. The results show that the doped state induces a slight dip in the SPR reflectivity curves, suggesting that the GO/PEDOT/PSS electrode is highly reactive in the PBS buffer. The PEDOT/PSS electrode has a lower peak absorption in the wider wavelength range than the GO/PEDOT/PSS electrode, as demonstrated in Figure 2.8. (d).

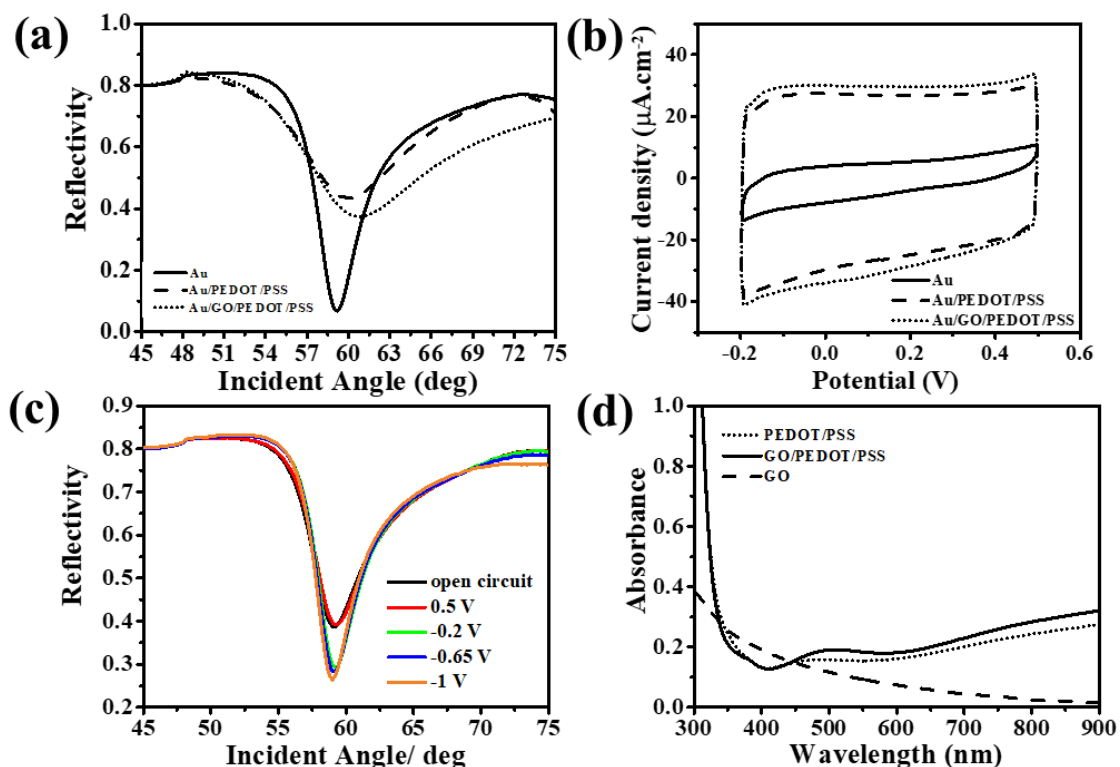


Figure 2.8 (a) SPR reflectivity curves on gold substrate in 10 mM PBS solution for bare, PEDOT/PSS substrate, and GO/PEDOT/PSS substrate, (b) CV responses of bare gold substrate, PEDOT/PSS substrate, and GO/PEDOT/PSS substrate in contact with 10.0 mM PBS solution, (c) SPR reflectivity intensities of the GO/PEDOT/PSS substrate with various constant potentials and open circuits applied, (d) UV-vis absorption spectra of GO, PEDOT/PSS, and GO/PEDOT/PSS electrode.

#### **2.4.3.2 STRUCTURE OF EC-SPR BIOSENSOR BASED ON GO/PEDOT/PSS SUBSTRATE**

Figure 2.9 (a) shows the simultaneous SPR kinetic study in the fabrication of the GO/PEDOT/PSS-based immunoassay for the assay of IgG, which corresponds to the chart model displayed in Figure 2.6. The reflectivity of GO/PEDOT/PSS/gold substrate in PBS buffer is employed as the starting point for study the SPR kinetic. The EDC/NHS solution is added to introduction of the -COOH group from GO linked to the GO/PEDOT/PSS electrode. An excess EDC/NHS is removed from the substrate by washing it with PBS solution. The activated surface is then injected with IgG-antibodies solution. The amide attachment of anti-IgG onto the active surface increased SPR reflectivity once again. PBS solution is used to rinse the chip once again. To inactivate the remaining free binding sites, the EA-HCl solution is employed. This avoids nonspecific adsorption of other chemicals by detecting human IgG, which would otherwise damage the sensor. The excess EA-HCl is rinsed before the determination of human IgG. After injecting human IgG, the reflectivity increased, which was linked to the selective binding of IgG-antibodies and human IgG. The electrode is washed with PBS solution for 10 minutes. The dissociation of physically adsorbed IgG resulted in a decline in SPR reflectivity. The reflectivity became stable after the nonspecific binding of IgG is eliminated. These results also imply that GO might be used in a human IgG test using the GO/PEDOT/PSS sensor. In the absence of GO, no change in SPR reflectivity is seen after activation of the PEDOT/PSS electrode surface by the EDC/NHS mixture solution (Figure 2.9 (b)). The GO in the GO/PEDOT/PSS electrode is necessary for the intermolecular immobilization of IgG-antibodies, which leads to improved sensor stability.

The chemical attachment of the PEDOT/PSS electrode prevents anti-IgG desorption from the electrode (Figure 2.9). (b).

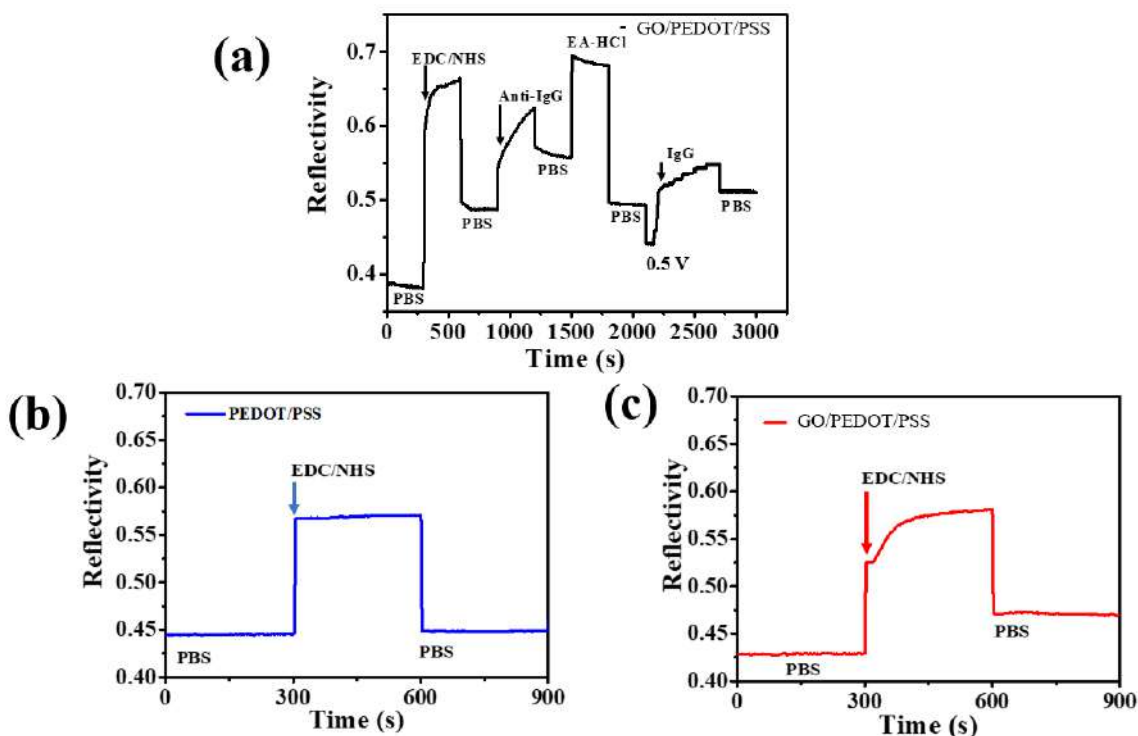


Figure 2.9 (a) Sensorgram of a GO/PEDOT/PSS-based biosensor during construction and assay 10  $\mu\text{g/mL}$  IgG with used potential at 0.50 V. The kinetic reaction of SPR during PEDOT/PSS formulation without (b) and with GO (c) after injection of the EDC/NHS mixture as a coupling reagent for 5 min and rinsing with PBS buffer.

#### 2.4.3.3 THE ASSAY OF IgG BY GO/PEDOT/PSS ELECTRODE

Two types for the assay of IgG antigen employing EC-SPR chip are investigated using the EC-SPR setup. The first type demonstrated that the developed GO/PEDOT/PSS-based immunoreaction achieved the maximum assay intensity of IgG without applied

potential or open circuit when compared to immunosensors fabricated using 3-MPA/gold, GO/gold, and PEDOT/PSS/gold electrodes. The second type is the electrochemical monitor of the suggested EC-SPR immunoassay by using several applied potentials (-1.0, -0.65, -0.20, and 0.50 V) before introducing IgG antigen solution. Open-circuit recognition is utilized as a reference to examine the impact of varying potentials on the immunosensor's sensitivity. As a result, electrochemical modulation increased the performance of the GO/PEDOT/PSS-based immunoassay is shown in Table 2.1. The sensitivity of IgG biosensor is better under applied potential field more than -0.65 V compared to the open-circuit potential, but it is lowered (to about 19%) at the used potential below -1.0 V due to PEDOT/PSS shrinkage in the de-doped complex layer. The sensitivity is slightly reduced to 3% when a constant potential of -0.65 V is used. The utilized constant field of -0.20 V provided 10 % of the sensitivity enhancement. It is observed that at a potential of 0.50 V, the maximum sensitivity is obtained. The sensitivity of immunosensor is increased by 24 % when an electrochemical constant potential of 0.5 V is applied. The LOD of our suggested immunosensor is 0.35 g/mL during an applied potential at 0.5 V, which is adequate for detecting the IgG concentration in the normal human body. This suggests that the immunosensor's electrochemically measured potential changed the immunoreaction performance of IgG antibodies and IgG antigen on GO/PEDOT/PSS. The GO/PEDOT/PSS SPR chip has a larger quantity of IgG. At a high electrochemical potential, a binding reaction is expected, resulting in a larger shift in SPR reflectivity.



**Table 2.1.** Comparison of the sensitivity of all immunosensors under different constant potentials

Film	Applied potential (V)	Sensitivity (mL $\mu\text{g}^{-1} \text{cm}^{-2}$ )
3-MPA	-	$2.56 \times 10^{-3}$
GO	-	$4.64 \times 10^{-3}$
PEDOT/PSS	-	$4.64 \times 10^{-3}$
GO/PEDOT/PSS	open circuit	$4.96 \times 10^{-3}$
GO/PEDOT/PSS	-1.0	$4.00 \times 10^{-3}$
GO/PEDOT/PSS	-0.65	$4.80 \times 10^{-3}$
GO/PEDOT/PSS	-0.20	$5.44 \times 10^{-3}$
GO/PEDOT/PSS	0.50	$6.08 \times 10^{-3}$

The GO/PEDOT/PSS substrate is investigated without electrochemical control. As shown in Figure 2.10 (a), the assay of IgG is tested on 4 changed electrodes with varied levels of human IgG for 1.0, 2.5, 5.0, and 10  $\mu\text{g}/\text{mL}$ . The SPR response is linearly proportional to IgG concentration in all of the curves. At various IgG concentrations, the sensitivities and SPR curves of the GO/gold, PEDOT/PSS/gold, and GO/PEDOT/PSS/gold biosensors are contrasted to those of a conventional SPR biosensor fabricated with a 3-MPA solution. The same process is used to produce an immunosensor on each film as it used on the GO/PEDOT/PSS electrode. When IgG-antibodies and human IgG are bound to the GO/PEDOT/PSS electrode, the SPR response is higher than in the GO/gold,

PEDOT/PSS/gold, and 3-MPA/gold-based biosensors (Table 2.1). The proposed biosensor is 7 % more sensitive than the GO/gold and PEDOT/PSS/gold biosensors, and 94 % more sensitive than the 3-MPA-based biosensor. This finding implies that the GO/PEDOT/PSS layer is more effective in detecting human IgG.

Figure 2.10 (b) illustrates designs of the reflectivity shift through assay with various concentrations of IgG with applied different constant fields of 0.50, -0.20, -0.65, and 1.0 V, as well as at the without applied potential. The linear curve improve in reflectance as a role of human IgG intensity is also seen at various applied potentials. At the same IgG concentration and upper applied constant potentials, the SPR signal is observed to be larger than at the without applied potential. As a result, electrochemical monitoring increased the binding ability of the GO/PEDOT/PSS-based biosensor.

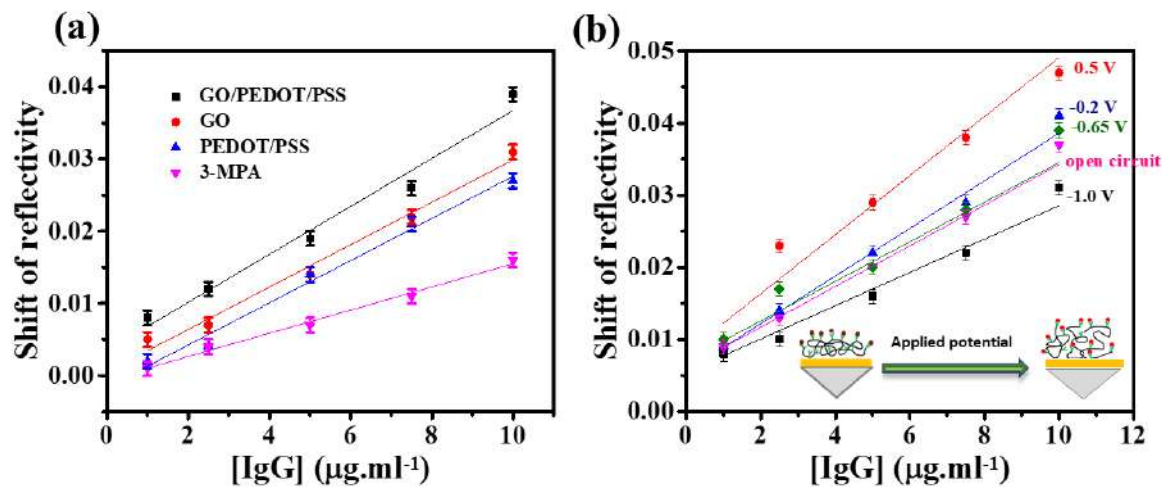


Figure 2.10 (a) Reflectivity change as a purpose of IgG concentration for immunosensors based on 3-MPA/gold, PEDOT/PSS/gold, GO/gold, and GO/PEDOT/PSS/gold without applied potential; (b) reflectance change as a role of IgG concentration for the developed biosensor based on GO/PEDOT/PSS at various applied potentials and without applied potentials.

The surface morphology and average roughness of the created GO/PEDOT/PSS platforms through surface-conjugated anti-IgG substrates may be connected to the improved sensitivity of the immunosensor under the used constant potentials. With different applied potentials, the film's morphology is expected to change. When the applied voltage is increased, the SPR dip angle is decreased and narrow, implying that the GO/PEDOT/PSS electrode is oxidized. The lowest sensitivity is found at 1.0 V due to a lesser number of anti-IgG on the electrode, whereas at 0.50 V, the maximum sensitivity is recorded because of the maximum number of surface-functionalized anti-IgG protruding into the analyte solution. An increase in the positive potential of the GO/PEDOT/PSS surface caused by doping could

also account for the enhanced sensitivity. The improved sensing surface may impact IgG binding on anti-IgG functionalized GO/PEDOT/PSS electrodes.

#### **2.4.3.4 KINETIC STUDY OF IMMUNOREACTION AT ELECTRODE SURFACE**

In the immunoreaction of GO/PEDOT/PSS sensor, human IgG and Anti-IgG antibodies emerge on the detecting surface. When surface-coupled anti-IgG comes into close contact with IgG in the PBS, the immunoreaction forms automatically. The sensitivity of the immunosensor is affected by the sensor's binding performance. As a result, the equilibrium association constant ( $K_A$ ) is used to define the affinity connections between functionalized anti-IgG and IgG. Furthermore, the kinetics of this procedure must be studied to determine dynamic and kinetic characteristics. During the binding process, our results are analyzed using a basic 1: 1 conjugation template that incorporates an immunoreaction containing of an anti-IgG antibody and an IgG molecule. The reflectivity of the SPR system ( $R_t$ ) is relational to the amount of immunoreaction, and at steadiness, the adsorptions, which include both selectivity and non-selectivity binding activities, reach a highest point and continue stable. The reflectivity also becomes constant ( $R_{eq}$ ) at this stage. After the addition of IgG solution, the association rate constant ( $k_a$ ) and  $K_A$  govern the binding process on our sensor. After continuous washing, dissociation is detected, which is regulated by the dissociation rate constant ( $k_d$ ). Table 2.2 shows the  $k_a$  and  $k_d$  acquired in our GO/PEDOT/PSS-based biosensor at various concentrations of IgG target. The observed decrease in  $k_a$  is revealed to be a purpose of the initial concentration of human IgG. The amount of interaction enhanced as

the quantity of human IgG reduced, indicating that IgG proteins have low amounts of molecular structure at low concentrations, signifying that movement to the sensor surface is unrestricted. When the amount of injected IgG is reduced, the  $k_d$  value changed significantly, although the  $K_A$  value increased. This suggests that the sensor has a strong affinity at low concentrations. Increases in  $k_a$  and  $K_A$  are observed with an increase in applied potential of the GO/PEDOT/PSS-based biosensor (Table 2.3).  $K_A$  is related to that detected at -1.0 V in open circuit, whilst  $K_A$  is similar to the amount studied at the utilized potential of -0.65 V. There is no considerable variation in  $k_d$  throughout each electrochemical control investigations. The greatest  $k_a$  and  $K_A$  values are revealed at a used potential of 0.50 V, implying the strongest attraction of immunocomplexes. This result is consistent by the immunosensor's sensitivity, as presented in Figure 2.10 (b) and Table 2.3. It is interesting to note that electrochemical control at 0.50 V can increase sensitivity while also influencing kinetics of the complex formation.

**Table 2.2** shows the  $k_a$  and  $k_d$  values determined from the designed GO/PEDOT/PSS biosensor at changed IgG concentrations.

<b>IgG concentration (<math>\mu\text{g/mL}</math>)</b>	<b><math>k_a</math> (<math>\text{M}^{-1} \text{s}^{-1}</math>)</b>	<b><math>k_d</math> (<math>\text{s}^{-1}</math>)</b>	<b><math>K_A</math> (<math>\text{M}^{-1}</math>)</b>
1.0	$1.79 \times 10^6$	$8.0 \times 10^{-4}$	$2.24 \times 10^9$
2.5	$4.60 \times 10^5$	$4.0 \times 10^{-4}$	$1.15 \times 10^9$
5.0	$2.87 \times 10^5$	$6.0 \times 10^{-4}$	$4.78 \times 10^8$
7.5	$2.02 \times 10^5$	$5.7 \times 10^{-4}$	$3.54 \times 10^8$
10	$1.35 \times 10^5$	$7.0 \times 10^{-4}$	$1.92 \times 10^8$

**Table 2.3**  $k_a$  and  $k_d$  values measured under electrochemical control from the designed GO/PEDOT/PSS-based biosensor at 10  $\mu\text{g/mL}$  target IgG.

<b>Applied potential (V)</b>	<b><math>k_a</math> (<math>\text{M}^{-1} \text{s}^{-1}</math>)</b>	<b><math>k_d</math> (<math>\text{s}^{-1}</math>)</b>	<b><math>K_A</math> (<math>\text{M}^{-1}</math>)</b>
open circuit	$1.35 \times 10^5$	$8.00 \times 10^{-4}$	$1.92 \times 10^8$
0.50	$2.34 \times 10^5$	$9.00 \times 10^{-4}$	$2.60 \times 10^8$
-0.20	$1.97 \times 10^5$	$8.50 \times 10^{-4}$	$2.32 \times 10^8$
-0.65	$1.74 \times 10^5$	$8.81 \times 10^{-4}$	$1.98 \times 10^8$
-1.0	$1.35 \times 10^5$	$7.70 \times 10^{-4}$	$1.75 \times 10^8$

When the sensor surface (solid phase) and aqueous phase are in equilibrium, the Freundlich model is employed to report on the distribution of the target IgG. Table 2.4 shows the  $K_F$  and the correlation coefficient ( $R^2$ ) for the adsorption investigation of target IgG onto the GO/PEDOT/PSS substrate with applied various constant potentials. The Freundlich model's correlation is represented by the  $R^2$  of the linear relationship.  $K_F$  increased as the applied potential increased, demonstrating that electrochemical stimulation enhanced the surface's adsorption capacity and ability, as well as the intensity of the adsorption process. The maximum  $K_F$  is observed with an applied potential at 0.50 V. This  $K_F$  represents the most successful human IgG binding method. Consequently, we suggest that the GO/PEDOT/PSS electrode may be electrochemically regulated to obtain maximal sensor affinity by applying a constant potential. The sensitivity and specificity of the designed GO/PEDOT/PSS-based biosensor are in high quality agreement, according to the findings of the kinetic research.

**Table 2.4** Freundlich's constant for human IgG binding of the GO/PEDOT/PSS-based biosensor

<b>Applied potential (V)</b>	<b><math>K_F</math></b>	<b><math>n</math></b>	<b><math>R^2</math></b>
open circuit	$2.31 \times 10^{-3}$	2.48	0.9973
-1.0	$1.03 \times 10^{-3}$	2.55	0.9728
-0.65	$1.25 \times 10^{-3}$	2.47	0.9795
-0.20	$3.20 \times 10^{-3}$	2.43	0.9801
0.50	$5.25 \times 10^{-3}$	2.34	0.9967

#### 2.4.4 CONCLUSION

We constructed an electrochemically controlled SPR biosensor based on GO/PEDOT/PSS platforms. The SPR and electrochemical characteristics of a GO/PEDOT/PSS film are studied on a sensing platform, with GO providing excellent electroreactivity as well as a surface-COOH group. An EC-SPR system involves for real-time observing of reflectivity shifts through the electrochemically polymerization of the GO/PEDOT/PSS electrode, as well as investigation of the redox states of the polymer structure on a gold electrode. For the selective assay of IgG, the GO/PEDOT/PSS electrode is attached with anti-IgG. The LOD and sensitivity are investigated by modifying the shape of the GO/PEDOT/PSS electrode with various applied fields. The sensitivity of immunosensor is greatly impacted by the applied potentials. After an applied constant



potential of 0.5 V displayed a great linear calibration curve with a LOD of 0.35  $\mu\text{g/mL}$ . Our designed approach reveals a suitable, and specific interaction for detecting of human IgG level, and the established EC-SPR platform can be applied to the improvement of further clinical functions.

#### **2.4.5 REFERENCES**

- [1] S.A. Jost, L.-C. Tseng, L.A. Matthews, R. Vasquez, S. Zhang, K.B. Yancey, IgG, IgM, and IgA antinuclear antibodies in discoid and systemic lupus erythematosus patients, *The Scientific World Journal*, 2014(2014) 171028.
- [2] G. Vidarsson, G. Dekkers, T. Rispens, IgG subclasses and allotypes: from structure to effector functions, *Frontiers in Immunology*, 5(2014) 520.
- [3] H.H. Nguyen, J. Park, S. Kang, M. Kim, Surface plasmon resonance: a versatile technique for biosensor applications, *Sensors*, 15(2015) 10481-10510.
- [4] L. Zeni, C. Perri, N. Cennamo, F. Arcadio, G. D'Agostino, M. Salmona, A portable optical-fibre-based surface plasmon resonance biosensor for the detection of therapeutic antibodies in human serum, *Scientific Reports*, 10(2020) 11154.
- [5] M. Pesavento, L. De Maria, D. Merli, S. Marchetti, L. Zeni, N. Cennamo, Towards the development of cascaded surface plasmon resonance POF sensors exploiting gold films and synthetic recognition elements for detection of contaminants in transformer oil, *Sensing and Bio-Sensing Research*, 13(2017) 128-135.
- [6] S. Shi, L. Wang, R. Su, B. Liu, R. Huang, W. Qi, A polydopamine-modified optical fiber SPR biosensor using electroless-plated gold films for immunoassays, *Biosensors and Bioelectronics*, 74(2015) 454-460.

- [7] M.M. Abdi, L.C. Abdullah, A.R. Sadrolhosseini, W.M. Mat Yunus, M.M. Moxsin, P.M. Tahir, Surface plasmon resonance sensing detection of mercury and lead ions based on conducting polymer composite, *PloS one*, 6(2011) e24578-e.
- [8] P. Suvarnaphaet, S. Pechprasarn, Graphene-based materials for biosensors: A Review, *Sensors*, 17(2017) 2161.
- [9] M. Donarelli, L. Ottaviano, 2D Materials for gas sensing applications: A review on graphene oxide, MoS<sub>2</sub>, WS<sub>2</sub> and phosphorene, *Sensors*, 18(2018) 3638.
- [10] V.P. Jain, S. Chaudhary, D. Sharma, N. Dabas, R.S.K. Lalji, B.K. Singh, Advanced functionalized nanographene oxide as a biomedical agent for drug delivery and anti-cancerous therapy: A review, *European Polymer Journal*, 142(2021) 110124.
- [11] S.S. Hinman, K.S. McKeating, Q. Cheng, Surface plasmon resonance: material and interface design for universal accessibility, *Analytical chemistry*, 90(2018) 19-39.
- [12] A. Baba, P. Taranekar, R.R. Ponnampati, W. Knoll, R.C. Advincula, Electrochemical surface plasmon resonance and waveguide-enhanced glucose biosensing with N-alkylaminated polypyrrole/glucose oxidase multilayers, *ACS applied materials & interfaces*, 2(2010) 2347-2354.
- [13] J. Golden, M.D. Yates, M. Halsted, L. Tender, Application of electrochemical surface plasmon resonance (ESPR) to the study of electroactive microbial biofilms, *Physical Chemistry Chemical Physics*, 20(2018) 25648-25656.

## **CHAPTER 3**

### **TRANSMISSION SURFACE PLASMON RESONANCE BASED SENSORS**

#### **3.1 A GRAPHENE OXIDE-BASED TRANSMISSION SURFACE PLASMON RESONANCE BIOSENSOR FOR DETECTION OF HUMAN IgG**

##### **3.1.1 INTRODUCTION**

SPR technique is frequently used to describe and analyze ultra-thin films, as well as to investigate surface attachment, biomolecule interaction, and surface kinetics [1]. SPR excitation may be achieved using a variety of grating configurations. The system's versatility and simplicity make grating-based SPR a significant research area [2]. Recently, SPR excitation is demonstrated to improve light transmission through hole arrays or grating substrates. The usage of commercial digital versatile disc (DVD-R) recordings covered with a thin gold coating is of interest [3]. The TSPR of light transmitted through this gold grating substrate must have a sharp and narrow peak in the visible light region. The TSPR wavelength is defined by the pitch of the grating and the angle of incidence. Recently, it was reported that in the diffraction of the gold grating film, diffraction-based surface-enhanced transmission on the order of  $\pm 1$  is measured [4]. Light transmission is dependent on the uncoupling of surface plasmons, which are generated and confined to the metal's surface. As a result, TSPR spectroscopy is high sensitivity to the area of refractive index close to the metal/dielectric interaction, making it an important approach for optical detection. The

sensitivity is primarily determined by the surface structure utilized to link the stimulation of the near-field surface plasmon (SP) and the decoupling of the far-field free propagating light [5]. In this work, we studied at whether the TSPR signal might be improved further by modifying the surface pattern of the gold grating using GO (it is known that the transmission enhancement through the gold grating substrate).

### **3.1.2 EXPERIMENTAL FEATURES**

#### **3.1.2.1 CHEMICALS AND MATERIALS**

GO powder was synthesized using the modified Hummer method. Anti-IgG, human IgG, 0.20 M ethanolamine hydrochloride (EA-HCl), phosphate buffered saline tablets (10 mM PBS, pH 7.4), cysteamine 95% were obtained from Sigma Aldrich (USA). 1-Ethyl-3-(3-dimethylaminopropyl)-carbodiimide hydrochloride (EDC) and N-hydroxysuccinimide (NHS) were obtained from Tokyo Chemical Industry and Wako Pure Chemical Industries (Japan), respectively.

#### **3.1.2.2 INSTRUMENTATION**

The TSPR configuration was done in collinear geometry. A convex lens by a focal length of 150 mm (Newport Corporation, Irvine, CA, USA) was used to collimate white light with a halogen source (model LS1; Ocean Optics, Dunedin, FL, USA). The resultant beam was transmitted via a linear polarizer and recorded with s- and p-polarized light prior to being used to illuminate the grating substrate via a hole with a diameter of 2 mm. For manual alignment, the sample was placed on a rotating test holder. A 600  $\mu\text{m}$  optical fiber was used to capture the transmitted light, which was then recorded using a Fiberoptic Spectrometer

(SD2000; Ocean Optics). For all determination, information storage, and processing, OP Wave software was utilized.

### 3.1.2.3 SUBSTRATE PREPARATION

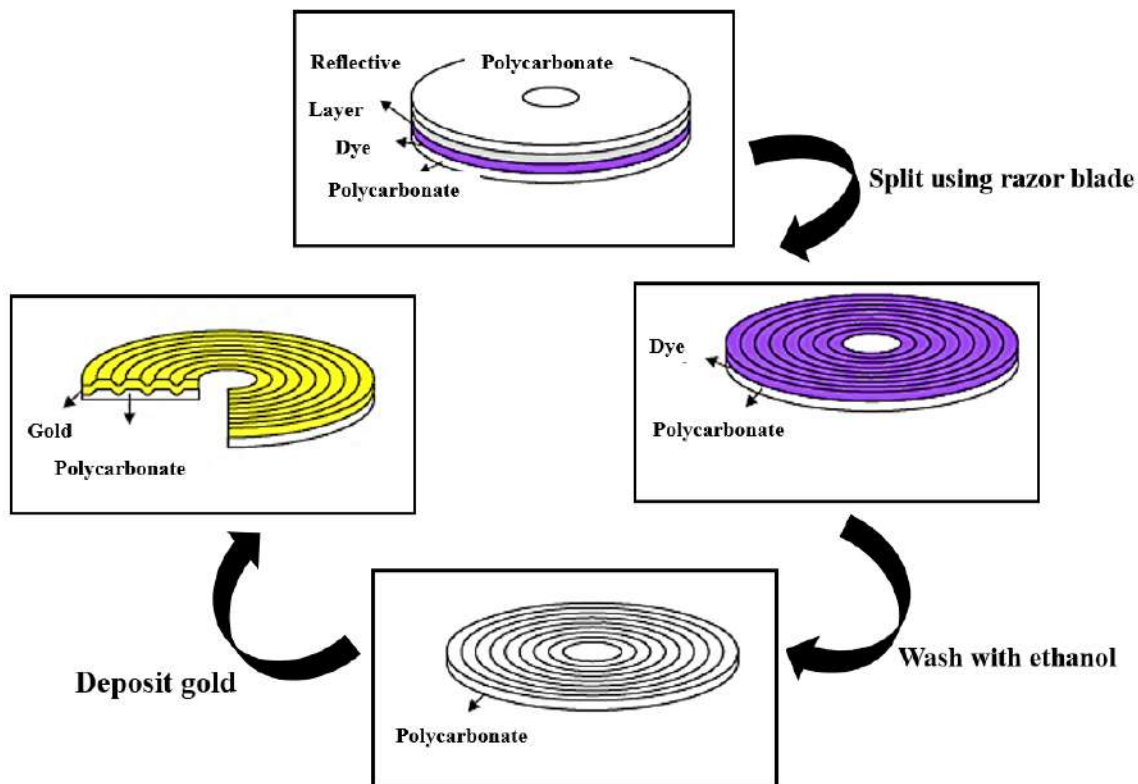


Figure 3.1 showing construction of gold gratings.

The diffraction grating pattern in this study was a gold-coated DVD-R grating substrate. The slotted polycarbonate components were removed from the polymer covering when the DVD-R was split into various pieces. To remove the dye layer on the slotted polycarbonate side, wash all substrate sheets with strong nitric acid for 5 minutes. The substrate was then washed twice with ethanol for 15 minutes and deionized water for 15 minutes. Finally, the pure N<sub>2</sub>

is used to air-dry the transparent grating substrate. A gold-coated TSPR grating substrate is made by vacuum evaporating a 3 nm chromium layer and a 47 nm gold layer on a clean TSPR substrate [6].

#### **3.1.2.4 FABRICATION OF IMMUNOSENSOR**

Following the immobilization of the GO sheath, the TSPR biosensor for the assay of human IgG was prepared. After establishing a baseline of TSPR in PBS, a 10-minute injection of a 1: 1 aqueous solution of EDC/NHS was used to activate the -COOH unit on the GO surface to N-hydroxy succinimide ester. After injecting the PBS solution as a wash solution, 100  $\mu\text{g/ml}$  anti-human IgG was added for 10 minutes. After washing with PBS, ethanolamine hydrochloride buffer (EA-HCl) was immersed for 10 minutes to prevent non-specific interaction by neutralizing the residual NHS groups that had not responded prior to detection. Figure 3.2 depicts the fabrication process for the GO-based biosensor for the assay of target IgG.

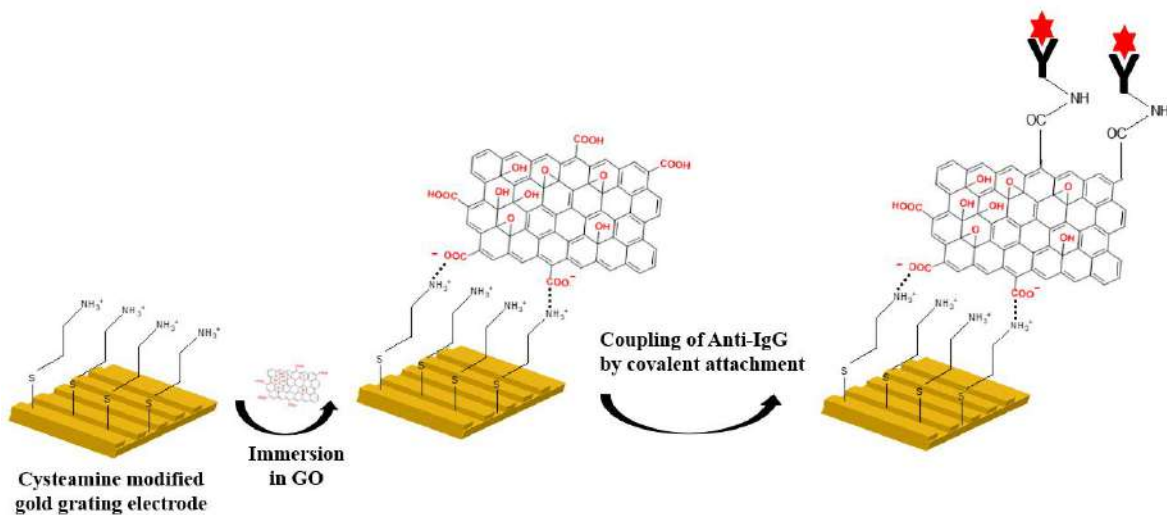


Figure 3.2 Schematic illustration of the building of an immunosensor based on GO for the assay of human IgG.

### 3.1.2.4 CONSTRUCTION OF 11-MERCAPTOUNDECANOIC ACID (11-MUA) FOR THE ASSAY OF HUMAN IgG

A thin layer of 11-MUA on the Au substrate was made by self-assembly of a single layer. The clean Au film was immersed in 10 mM 11-MUA in ethanol solution for 4 h at room temperature. After removing the template from the solution, it was washed with ethanol and deionized water in several times. After rinsing, the substrate was dried with a flow of pure N<sub>2</sub>. The 11-MUA thin layer on the gold substrate was used to make a biosensor-based self-assembled monolayer (SAM) of 11-MUA with a process similar to GO fabrication for the determination of human IgG. Figure 3.3 depicts a diagram representation of the building of a 11-MUA-based biosensor for the assay of human IgG.

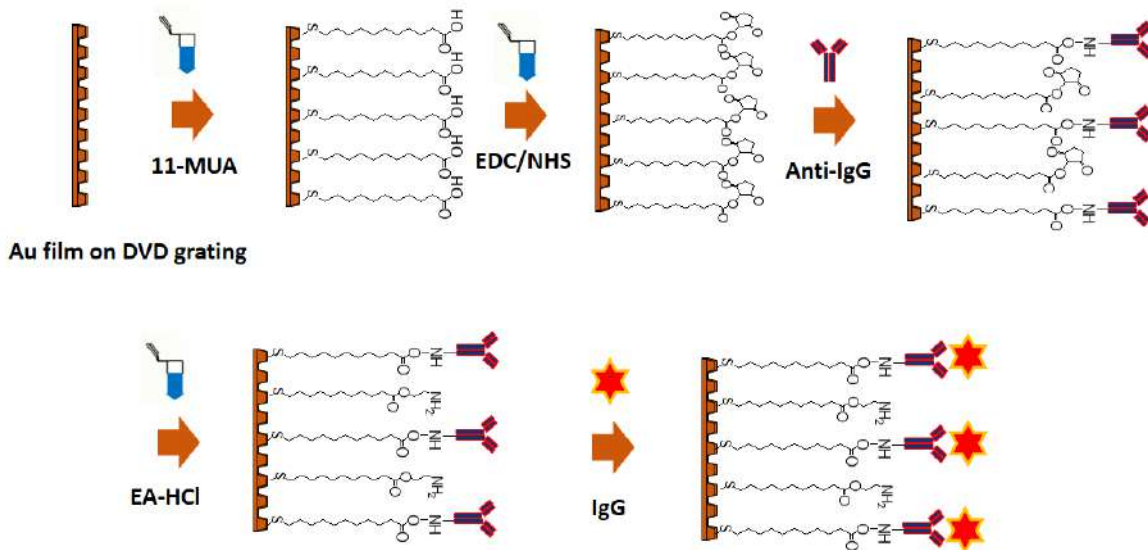


Figure 3.3 Schematic depiction of the building of an 11-MUA-based immunosensor for detecting human IgG.

### 3.1.3 RESULTS AND DISCUSSION

The original p-polarization spectrum was subtracted from the s-polarization spectrum to generate the TSPR spectrum utilized in this study. Figures 3.4 (a) and 3.4 (b) illustrate the TSPR response of the gold-coated DVD-R array base and GO gold-coated DVD-R array substrate as a different of incident angle from 0 to 40° (b). Distinct TSPR peaks are seen, with wavelengths ranging from 480 to 770 nm, depending on the correlation between the incident light wave vector and the vector modified surface plasmon wave vector on the lattice [7]. When the incidence angle of light varies from 0° to 35°, the TSPR intensity increases. When the incidence angle of the light is rotated above 40°, the intensity decreases. The strongest SPR peak in the T-SPR spectrum at 35° is at 770 nm.



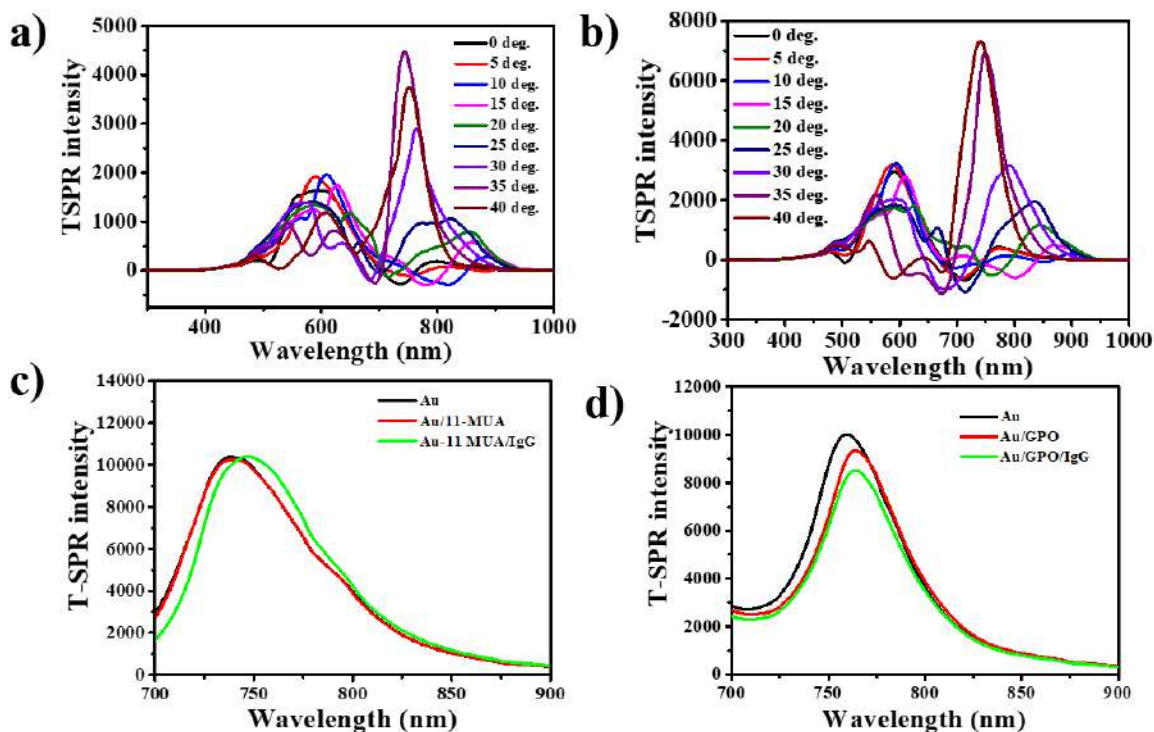


Figure 3.4 (a) The TSPR response of gold-coated grating pattern as a part of incident angle from 0 to 40° (b) The TSPR response of GO-gold-coated grating pattern as a part of incident angle from 0 to 40° (c) TSPR spectra of 11-MUA/gold grating film before and after detection of IgG and (d) TSPR spectra of GO/gold grating pattern before and after the detection of IgG.

### PREPARATION OF A GO-BASED TSPR BIOSENSOR FOR THE ASSAY OF HUMAN IgG

The GO-based immunosensor's sensitivity is compared to that of a conventional system. In this work, 11-MUA was employed to build a monolayer based on the self-assembled immunosensor, which served as the reference system. Figures 3.5(a) and (b) demonstrate the TSPR reactions for detecting human IgG on the anti-human IgG-MUA system versus the anti-human IgG/GO membrane, respectively. When compared to the conventional MUA

method, the correlation between the change in TSPR intensity and IgG levels on GO/Au films exhibited greater sensitivity. The association between the change in transmission intensity and human IgG interaction on Anti/IgG/GO/gold film is more sensitive than the 11-MUA system, with a dynamic range of 2.5-10  $\mu\text{g/mL}$  (Figure 3.6).

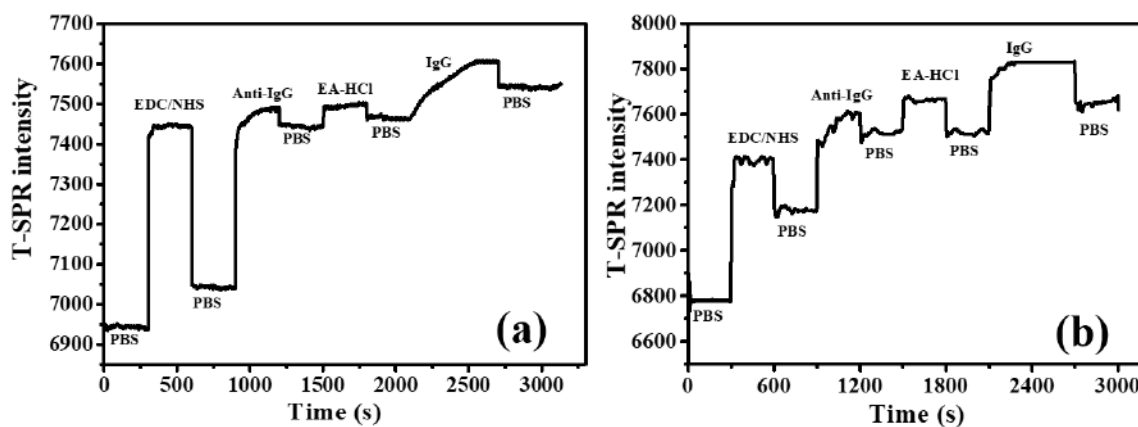


Figure 3.5 TSPR responses during the building of 11-MUA-based immunoassay for detecting 10  $\mu\text{g/mL}$  human IgG and (b) TSPR responses during the fabrication of a GO-based immunosensor for detecting 10  $\mu\text{g/mL}$  human IgG.

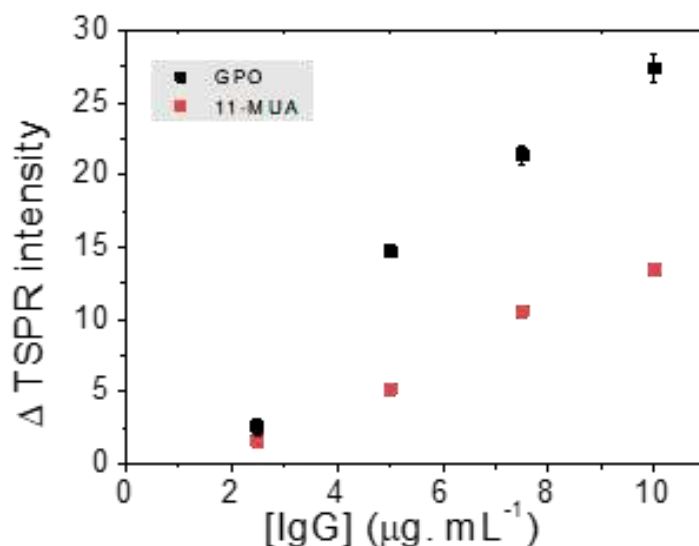


Figure 3.6 Calibration graph of different concentration human IgG and TSPR response during human IgG binding to anti-IgG/GO and anti-IgG/11-MUA system.

### 3.1.4 CONCLUSION

The capability, sensitivity, and applicability of TSPR technique for studying the characteristics of GO film and detecting human IgG have been established. TSPR measurements are used to study the in-situ immobilization of anti-human IgG and its immunoreaction with human IgG. The intensity of TSPR improved as human IgG levels increased. The GO/gold binding model employs the conventional 11-MUA system. We conclude that this approach may be used to investigate the interactions of biomolecules in many systems, and diagnostic tools in a variety of forms can be constructed.

## **3.2 TRANSMISSION SURFACE PLASMON RESONANCE IMAGING FOR DETECTION OF CREATININE**

### **3.2.1 INTRODUCTION**

Because high electric fields create intense and narrow spectra in the visible near infrared range, TSPR technique has become an interesting issue [8]. In this work, we studied the enhancement of TSPR characteristics based on the grating pattern of a DVD-R coated with a thin gold film and used this development for multiple applications including biosensors and adjustable TSPR due to the flexibility and simplicity of the technology [9]. The Hiller group published the first diffraction-based tracking TSPR dispersion image through a gold-plated grating arrangement in 2013 [10]. This picture shows a dense collection of TSPR spectra as a function of wavelength and incidence angle. It may be utilized to define plasma modes at the coupling and decoupling interfaces that are connected to diffraction orders. Previously, plasmonic nanoparticles based on localized surface plasmon resonance (LSPR) has been utilized to stimulate and modify the electric field between dielectric and metal interface to improve the signal of such TSPR templates [11, 12]. In this research, we investigate the impact of silver nanoparticles (AgNP) near-field LSPR on the far-field TSPR of gold grating substrates. The increased coupling is sensitive to the natural environment and may be exploited for creatinine detection since the dipole plasmon resonance wavelength in the AgNPs is near to the transmitting surface plasmon resonance wavelength of the gold grating substrate.

### 3.2.2 EXPERIMENTAL

#### 3.2.2.1 INVESTIGATION OF SYSTEM FOR TSPR IMAGE ACQUIREMENT

The camera (2084×2084 pixel image matrix, Zyla 5.5 sCMOS camera, Andor Technology Ltd.) and the adjustable liquid crystal filter (LCTF) (VariSpec, PerkinElmer, Inc.) are used to generate the TSPR image and signal. Figure 3.7 depicts a photograph of the TSPR imaging system. The picture capture exposure duration is 0.25 s. There are more than 200 pixels of average transmission intensity.

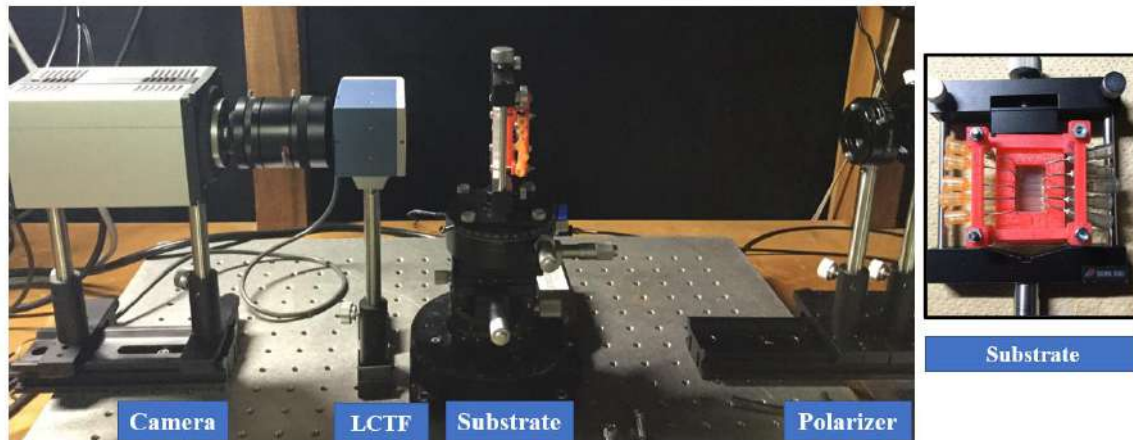


Figure 3.7 Photograph of the T-SPR imaging system.

#### 3.2.2.2 TSPR SUBSTRATE PREPARATION

Use sodium salt of 3-mercaptopropionate to functionalize the gold-coated grating substrate before applying 5 layers of poly (diallyldimethylammonium chloride)/poly (4 styrene sulfonate) (PDADMAC/PSS) film. Before cleaning the platform, inject the colloidal AgNP solution into the Teflon battery for 15 minutes to deposit the AgNPs on the surface of the functionalized gold-coated grating pattern (Figure 3.8).

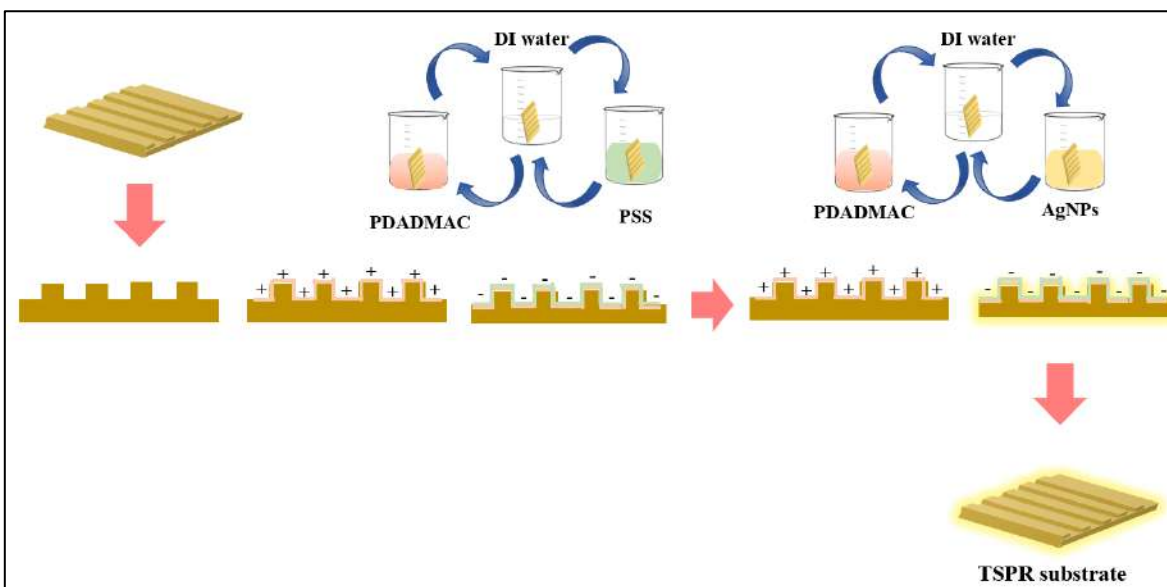


Figure 3.8 Schematic illustration representing the gold-coated grating/PDADMAC/PSS (10 bilayers)/PDADMAC/AgNPs (5 bilayers)/PDADMAC/PSS layer-by-layer (LBL) film assembled for the creatinine detection on gold grating substrate.

### 3.2.3 RESULTS AND DISCUSSION

The TSPR signal of gold-coated grating (50 nm) and gold-coated grating/PDADMAC/PSS (10 double layers)/PDADMAC / AgNPs (5 double layers)/PDADMAC/PSS at an incidence angle of  $0^\circ$  to  $40^\circ$  are collected at 500 to 950. For TSPR excitation wavelengths between, the angle of incidence is  $0^\circ$  to  $40^\circ$ , as shown in Figure 3.9. Inset demonstrates TSPR excitation wavelength versus angle of incidence for a gold-coated grating substrate.

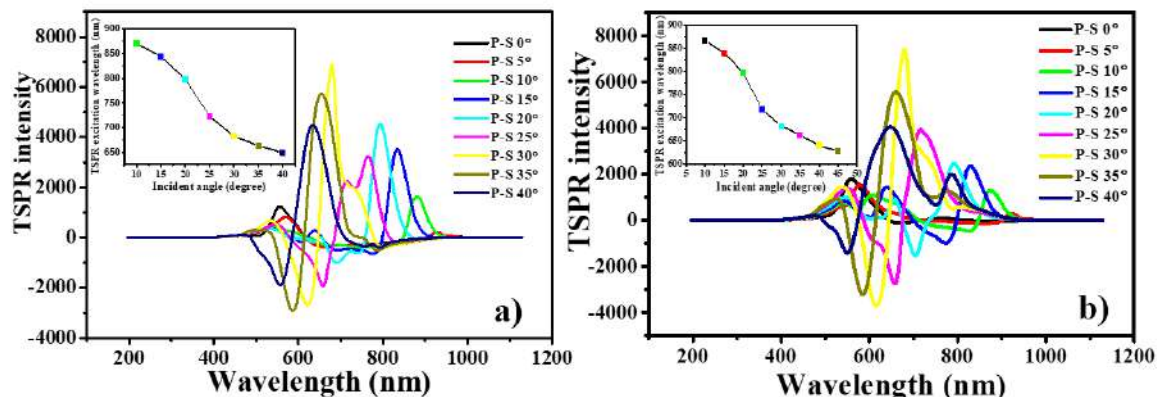


Figure 3.9 TSPR spectra of a gold-coated imprinted grating platform and gold-coated grating/PDADMAC/PSS (10 bilayers) / PDADMAC/AgNPs (5 bilayers)/PDADMAC/PSS at incident angles of  $0^\circ$  to  $40^\circ$ .

We deposited AgNPs on PDADMAC/PSS functionalized gold film substrates to observe the influence of near-field LSPR on the TSPR phenomena. As shown in Figure 3.10, the peak intensity of TSPR decreased after deposition on PDADMAC/AgNPs. Next, 1mM creatinine is injected onto a PDADMAC/AgNPs-PDADMAC/PSS film. As Figure 3.10, a significant decrease in the intensity of TSPR is observed, suggesting that creatinine is closely related to AgNPs.

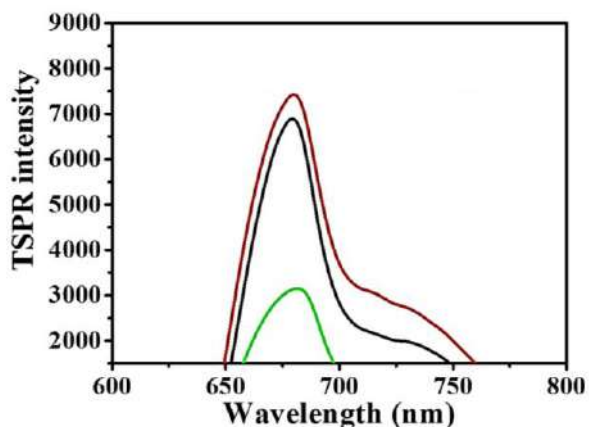


Figure 3.10 The TSPR curve of a gold-coated grating platform (black-line), after the functionalization of PDADM/AgNPs on PDADM/PSS film (red-line), and after the injection of creatinine on the gold-coated grating/PDADM/PSS/AgNPs-PDADM/PSS (green-line).

Since the intensity of TSPR varies with creatinine exposure, the TSPR-i system is used to measure the typical dependence of creatinine concentration. The 3-channel microfluidic TSPR platform is fabricated by assembling the 3-channel microfluidic channel on the PDADM/AgNPs-PDADM/PSS/gold-coated grating electrode. The preparation details of the 3-channel microfluidic TSPR cells are provided by Shin-Etsu Polymers. Figure 3.11 depicts the TSPR pictures for the simultaneous detection of various creatinine concentrations in PBS buffer and PBS buffer. The PBS creatinine buffer at concentrations of 1.0 and 10 mM without creatinine is injected into the microfluidic channel at the same time for 10 minutes, and then the PBS buffer is injected into all channels. The intensity of the TSPR image changes significantly with the presence of creatinine.



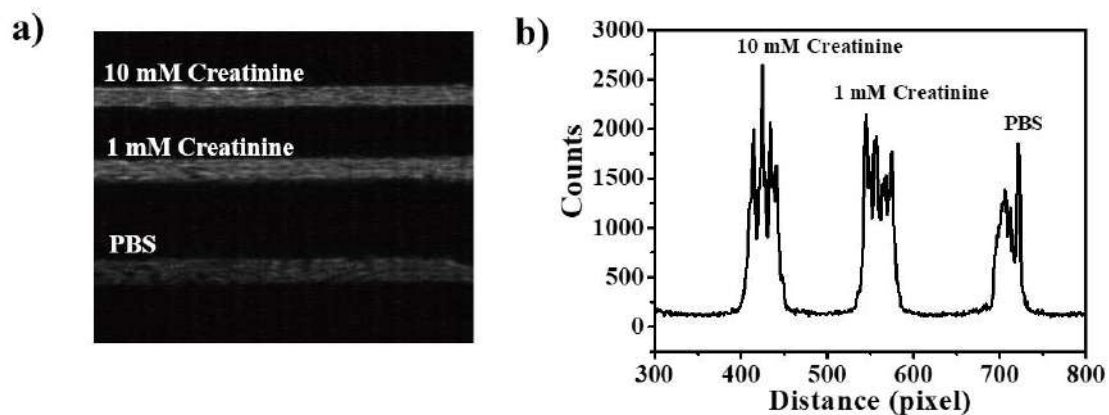


Figure 3.11 (a) The TSPR imaging and (b) The intensity of TSPR imaging of PBS, 1 mM creatinine and 10 mM creatinine on AgNPs response of a gold-coated grating platform, after the deposition of AgNPs, and after the injection of creatinine on the gold-coated grating/PDADMAC/PSS/PDADMAC/AgNPs.

### 3.2.4 CONCLUSION

In summary, TSPR-i is investigated using a three-channel microfluidic device. TSPR-i, a technique based on SPR propagation, is used to monitor the change of the surface plasmon resonance of the gold grating electrode and its surrounding environment in transmission mode. AgNPs, PDADMAC, and PSS are placed layer by layer on the surface of the gold thin film substrate for creatinine detection. A camera connected to the LCTF detects the TSPR-i signal. When AgNPs are deposited on a gold grating pattern, the intensity of TSPR-i drops and subsequently rises after 1 hour of incubation with creatinine. A simple approach of TSPR for real-time and label-free imaging systems is presented, which might be useful in clinical applications.

### 3.3 REFERENCES

- [1] C. Lertvachirapaiboon, A. Baba, K. Shinbo, K. Kato, A smartphone-based surface plasmon resonance platform, *Analytical Methods*, 10(2018) 4732-4740.
- [2] B.A. Prabowo, A. Purwidyantri, K.-C. Liu, Surface plasmon resonance optical sensor: a review on light source technology, *Biosensors*, 8(2018) 80.
- [3] S. Joseph, S. Sarkar, J. Joseph, Grating-coupled surface plasmon-polariton sensing at a flat metal–analyte interface in a hybrid-configuration, *ACS Applied Materials & Interfaces*, 12(2020) 46519-46529.
- [4] B.K. Singh, A.C. Hillier, Surface plasmon resonance enhanced transmission of light through gold-coated diffraction gratings, *Analytical Chemistry*, 80(2008) 3803-3810.
- [5] V.G. Kravets, A.V. Kabashin, W.L. Barnes, A.N. Grigorenko, Plasmonic surface lattice resonances: a review of properties and applications, *Chemical reviews*, 118(2018) 5912-5951.
- [6] R. Janmanee, A. Baba, S. Phanichphant, S. Sriwichai, K. Shinbo, K. Kato, In situ electrochemical-transmission surface plasmon resonance spectroscopy for poly(pyrrole-3-carboxylic acid) thin-film-based biosensor applications, *ACS Applied Materials & Interfaces*, 4(2012) 4270-4275.
- [7] T. Juagwon, C. Lertvachirapaiboon, K. Shinbo, K. Kato, T. Srihirin, T. Osotchan, A. Baba, Detection of human immunoglobulin G by transmission surface plasmon resonance using the in situ gold nanoparticle growth method, *IEICE Transactions on Electronics*, E102.C(2019) 125-131.

- [8] C. Lertvachirapaiboon, C. Pothipor, A. Baba, K. Shinbo, K. Kato, Transmission surface plasmon resonance image detection by a smartphone camera, *MRS Communications*, 8(2018) 1279-1284.
- [9] C. Lertvachirapaiboon, A. Baba, S. Ekgasit, K. Shinbo, K. Kato, F. Kaneko, Transmission surface plasmon resonance techniques and their potential biosensor applications, *Biosens Bioelectron*, 99(2018) 399-415.
- [10] W.-H. Yeh, A.C. Hillier, Use of dispersion imaging for grating-coupled surface plasmon resonance sensing of multilayer Langmuir–Blodgett films, *Analytical Chemistry*, 85(2013) 4080-4086.
- [11] J. Zhang, G. Kolhatkar, A. Ruediger, Localized surface plasmon resonance shift and its application in scanning near-field optical microscopy, *Journal of Materials Chemistry C*, 9(2021) 6960-6969.
- [12] Y. Hong, Y.-M. Huh, D.S. Yoon, J. Yang, Nanobiosensors based on localized surface plasmon resonance for biomarker detection, *Journal of Nanomaterials*, 2012(2012) 759830.

## CHAPTER 4

### ELECTROCHEMICAL-SURFACE PLASMON RESONANCE BASED SENSOR FOR DETECTION OF CREATININE

#### 4.1 INTRODUCTION

SPR is a great technique for studying analyte binding to functionalized surfaces and biomolecule immobilization [1, 2]. Creatinine is a biomarker used to evaluate kidney function and diagnose renal disease. Creatinine levels in the human body are elevated, indicating renal dysfunction [3-5]. In this work, we used the SPR technique to develop a novel approach for detecting creatinine utilizing starch-AgNPs on PPy thin films. The result demonstrates a distinct yellow to orange shift in the AgNPs solution with creatinine, suggesting high sensitivity owing to the AgNPs' local plasmon effect. The adsorption of AgNPs on the PPy film in the existence of creatinine enhances the change in SPR reflectance in the Kretschmann configuration [6, 7]. When injecting the mixed solution onto the thin film of PPy, the SPR reflectivity increased in a linear range of 10 to 1000 M with increasing creatinine level. The performance of the creatinine sensor with three SPR detection methods is investigated for comparison, namely one PPy membrane only, one PPy membrane with AgNP, and one PPy membrane with synthesized AgNP. The SPR sensor with synthetic AgNPs performs roughly four times better than substrates without synthetic AgNPs, with a LOD of 0.19 M. The proposed approach has the potential to be beneficial in clinical applications.

## **4.2 EXPERIMENTAL METHODS**

### **4.2.1 CHEMICALS AND MATERIALS**

L-ascorbic acid, creatinine, glucose, uric acid, phosphate-buffered saline tablets (10 mM PBS, pH 7.4), serum albumin, starch and silver nitrate were obtained from Sigma-Aldrich (USA). Pyrrole was obtained from the chemical industry in Tokyo (Japan). DI water was used to make all aqueous solutions.

### **4.2.2 EC-SPR EQUIPMENT**

SPR reflectivity is monitored using a laboratory-developed reduced total reflection (ATR) apparatus by a Kretschmann formation combine with a 3-electrochemical cell, as illustrated in Figure 4.1. A He-Ne laser at a wavelength of 632.8 nm is utilized as the excitation source. Vacuum evaporation is used to cover the gold-coated high refractive index glass substrate with 3 nm of chromium and 47 nm of gold. The gold chip is constructed on a Teflon cell and installed on a turntable for electrochemical polymerization and creatinine detection. The working electrode was an evaporated gold SPR chip (the working surface area was 0.63 cm<sup>2</sup>), the silver/silver chloride 3M NaCl as a reference electrode, and the platinum wire as a counter electrode was utilized for electropolymerization and electrochemical study. A potentiostat was used to measure the cyclic voltammogram (CV) (Hokuto Denko HZ-7000).

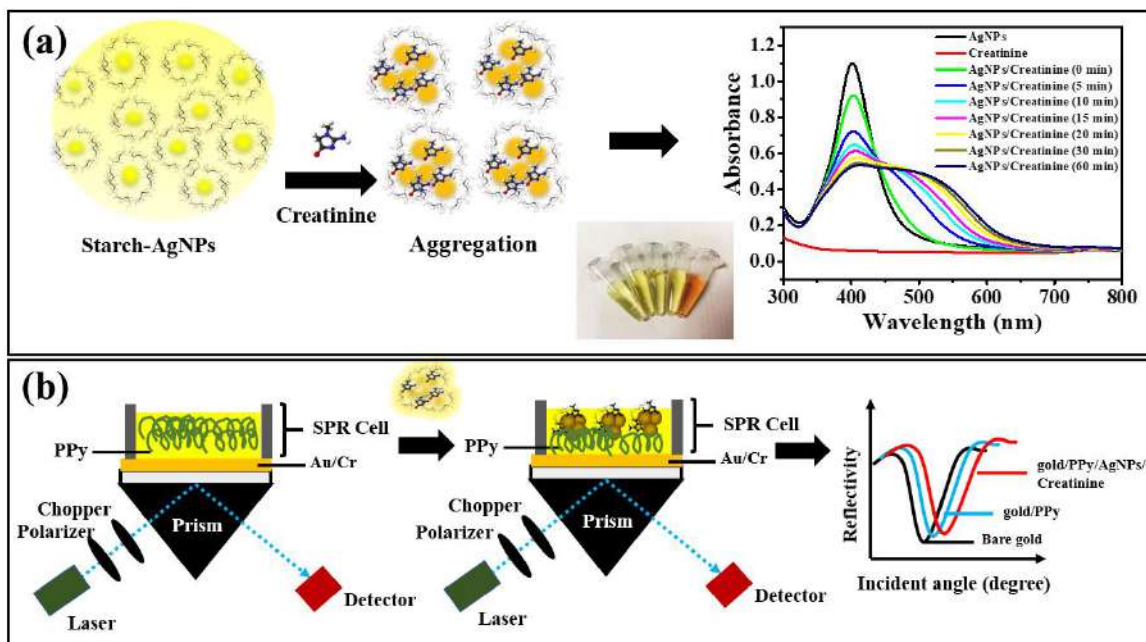


Figure 4.1 Schematic of the developed SPR sensor applying AgNPs on a PPy/gold film for the assay of creatinine.

#### 4.2.3 CONSTRUCTION OF POLYPYRROLE ELECTRODE-BASED SPR SENSOR FOR THE ASSAY OF CREATININE

The synthesis of the PPy polymer by electropolymerization process was made in the mixing 0.5 M pyrrole and 10 mM PBS solution (pH 7.4). The CV was used to electropolymerize PPy from -0.2 to 1.0 V for 3 cycles with a scan rate of 20 mV/s on high refractive index gold glass substrate.

## 4.3 RESULTS AND DISCUSSION

### 4.3.1 UV-VIS ABSORPTION STUDIES OF AgNPs-CREATININE STRUCTURE

To offer a quantitative measurement of creatinine, UV-Vis spectroscopy is used to monitor the aggregation of the AgNPs solution. The addition of 10 mM creatinine in AgNPs solution led to a decline in LSPR intensity at 400 nm and the formation of a new wide peak at about 550 nm, suggesting that the LSPR peak is slowly converted from distinct AgNPs at 400 nm in AgNPs solution aggregation (Figure 4.2 (a)). The peak of absorption around 400 nm decreases rapidly with increasing of time (Figure 4.2 (b)) and becomes almost saturated after about 30 min. Interestingly, the peak absorption ratio  $A_{550/400}$  nm increases linearly with time (Figure 4.2 (c)). Because of the negative -OH group of starch that adsorb on the structure of AgNPs during the synthesis process, starch plays as a stabilizing agent. Moreover, the -OH groups serve as a H-attachment with creatinine. Because the -NH<sub>2</sub> group of creatinine has a much higher binding affinity than the -OH group, and because creatinine is a tiny molecule, it can easily connect to AgNPs, this stabilization can be disrupted. After binding with creatinine, AgNPs are destabilized from starch, allowing AgNPs to combine with more molecules. The UV-vis spectrum confirms the expectation, and the following injection of creatinine resulted in an apparent color shift from yellow to orange.

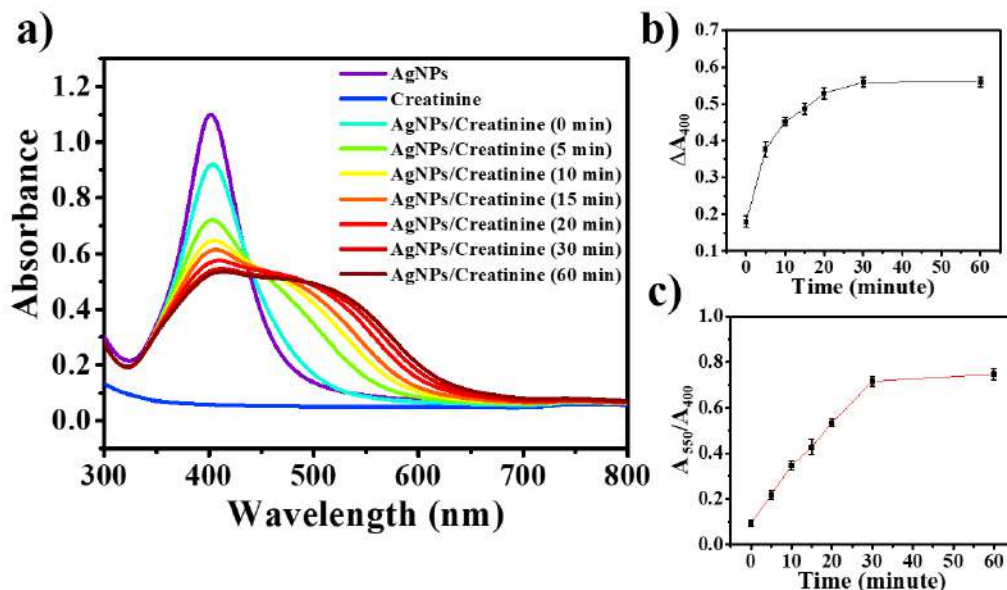


Figure 4.2 (a) UV-Vis spectrum of AgNPs, creatinine and AgNPs with different time after mixing creatinine from 0 to 60 minutes (b) Different absorption of LSPR at 400 nm from 0 to 60 minutes with time, and (c)  $A_{550\text{ nm}}/A_{400\text{ nm}}$  as different time, from 0 to 60 minutes after mixing AgNPs and creatinine.

### 4.3.2 FRABRICATION AND CHARACTERIZATION OF POLYPYRROLE ON GOLD FILM

0.05 M pyrrole monomer solution in 10 mM PBS solution is utilized for electropolymerization of the PPy layer on the gold/SPR electrode for 3 cycles at a voltage of -0.2 to 1.0 V and a scan rate of 40 mV/s. Figure 4.3 (a) depicts the CV characteristics of PPy electropolymerization onto a gold covered SPR substrate. The SPR kinetic study is shown in the inset for three cycles of electropolymerization of PPy at a set incidence angle of 58.5°. The oxidation peak current above 0.7 V increased with the electropolymerized of cycles,



suggesting that the PPy layer is formed on a gold-coated substrate. The improvement in SPR reflectivity in the Figure 4.3 (b) (inset) and the change in SPR dip angle in Figure 4.3 (b) both verified the creation of the PPy layer on the gold film (b).

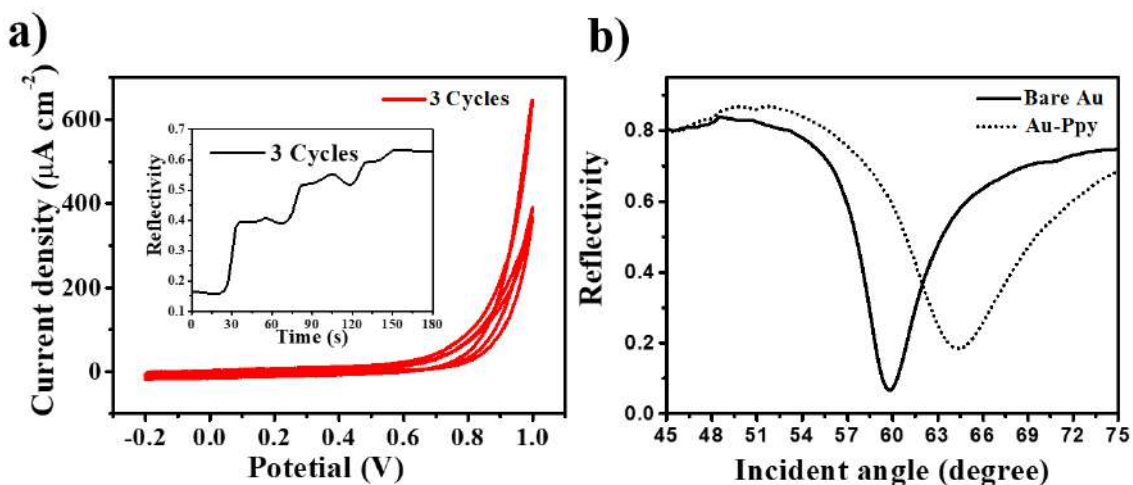


Figure 4.3 (a) CV curves for 3 cycles of electrodeposition of PPy onto gold SPR electrode and (inset) SPR curve for 3 cycles of eletropolymerization of PPy, (b) SPR curves for only gold and PPy/gold platform.

### 4.3.3 THE DETECTION OF CREATININE BY SURFACE PLASMON RESONANCE TECHNIQUE

On the PPy/Au substrate, Figure 4.4 (a) (black line) depicts the SPR response of position PBS solution, creatinine (green line), (red line) AgNPs solution, AgNP/creatinine solution after mixing time (0 minutes) (blue line), and AgNP and creatinine (30 minutes after mixing) (skyline). The combination of AgNP and creatinine increased SPR reflectivity more than AgNP and creatinine alone, as seen in the figure. At 30 minutes after mixing, AgNPs-

creatinine demonstrated the greatest rise in SPR refractive index. This suggests that combining AgNPs-creatinine with creatinine detection could enhance its accuracy. The concentration dependency of each example is displayed in Figure 4.4 (b) and (c). The SPR signal to creatinine concentration is linear in all curves. At varying concentrations of creatinine, compare the sensitivity and SPR signal of AgNPs/creatinine (0 minutes after mixing) and AgNPs/creatinine (after 30 minutes mixing) with detection of creatinine not including AgNPs. AgNPs/creatinine sensitivity is 4 % greater (30 minutes after mixing) than AgNPs/creatinine (after 0 minutes mixing) and 7 % higher than creatinine no added AgNPs. This finding shows that AgNPs/creatinine in PPy (after 30 minutes of mixing) detects creatinine more accurately. Table 4.1 summarizes each type of creatinine application potential.

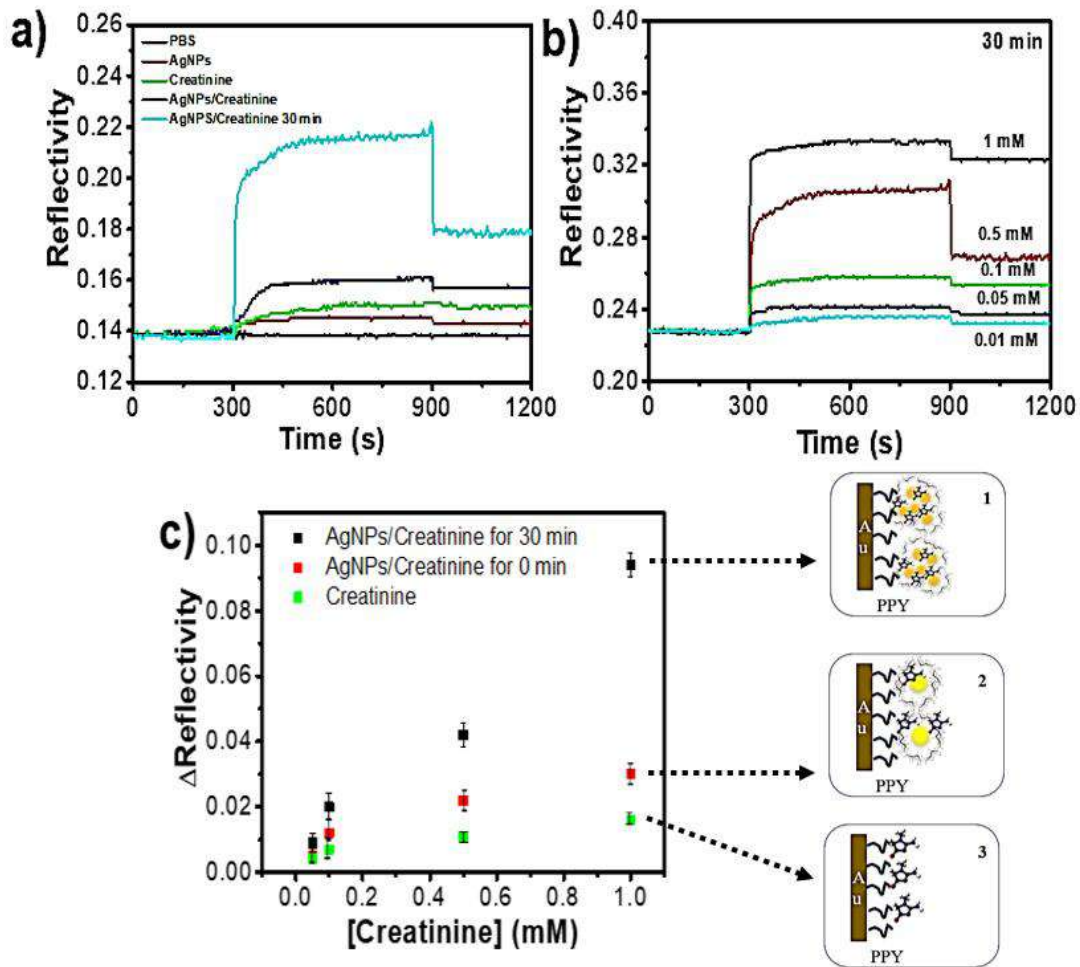


Figure 4.4 SPR response in AgNPs/creatinine (30 min) AgNPs/creatinine (0 min), AgNPs, and, PBS solution on the PPy/gold electrode, (b) AgNPs/creatinine (30 min), and (c) Three linear curves for the assay of creatinine present and absent AgNPs; the black, red, and green lines related to AgNPs/creatinine (30 min), AgNPs/creatinine (0 min), and creatinine solution, respectively.

**Table 4.1** The PPy, PPy/AgNPs and PPy/aggregated AgNPs based sensor with different creatinine concentrations.

<b>SPR sensors</b>	<b>Linear range (<math>\mu\text{M}</math>)</b>	<b>Sensitivity (<math>\text{cm}^{-2}\mu\text{M}</math>)</b>	<b>LOD (<math>\mu\text{M}</math>)</b>
PPy/Creatinine	50 to 1000	11.6	31.18
PPy/AgNPs/Creatinine	10 to 1000	21.2	2.53
PPy/aggregated AgNPs-Creatinine	10 to 1000	86.3	0.19

In the absence of creatinine, different additional compounds (such as, glucose albumin, ascorbic acid, and uric acid) are introduced to AgNP to test the selectivity of the proposed technique, as shown in Figure 4.5. 500  $\mu\text{L}$  of every component are increased to 500  $\mu\text{L}$  of AgNPs. A different color shift from yellow to orange may be seen in the existence of creatinine, but no substantial color variation can be seen in the existence of glucose, albumin, ascorbic acid, and uric acid. Additionally, when detecting AgNPs-creatinine mixes, the reflection properties of SPR only exhibit substantial changes, which might be attributed to the impact of AgNPs and creatinine aggregation. The results demonstrate that the probe is quite specific for creatinine detection.

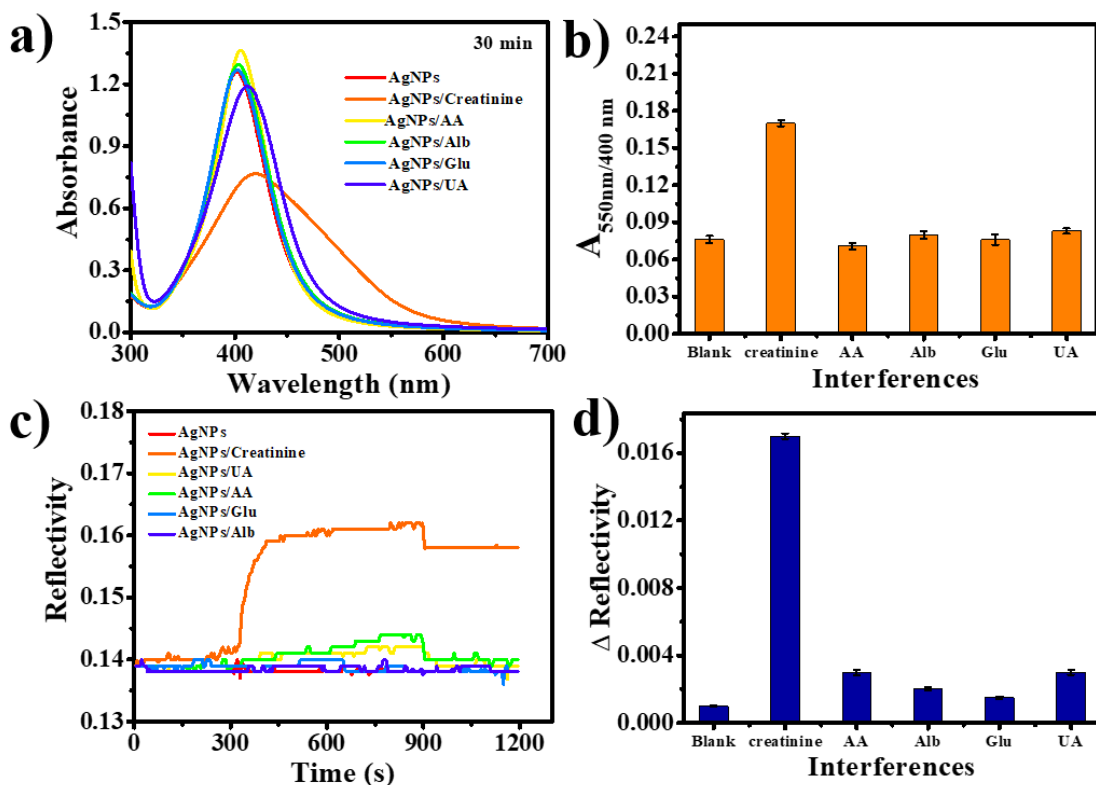


Figure 4.5 Interference study

Moreover, the adsorption of AgNPs-creatinine may be improved by changing the electrochemical potential at the PPy/Au electrode. The adsorption properties of AgNP at open circuit potential and constant applied potentials (-0.3, 0.3, and 0.5 V) controlled using EC-SPR technique are shown in Figure 4.6 (a). The positive applied potential clearly enhances AgNP adsorption, as shown by the results. Because AgNP is negatively charged, electrostatic contact should be a factor in the enhanced adsorption. The increase in the reflectance of EC-SPR is also seen using a positive potential for the detecting AgNPs/creatinine (30 minutes after mixing), as shown in Figure 4.6. (b). It should also be noted that when the potential gets more accurate, the AgNPs/creatinine adsorption rate will increase. Table 4.2 displays the

calculated  $k_a$ ,  $k_d$ , and  $K_A$ . Although  $k_d$  is somewhat greater when the greatest potential is used, there is no statistically significant difference in  $k_d$  in all cases. The greatest values of  $k_a$  and  $K_A$ , on the other hand, are found at an applied potential of 0.50 V, signifying the strongest specificity.

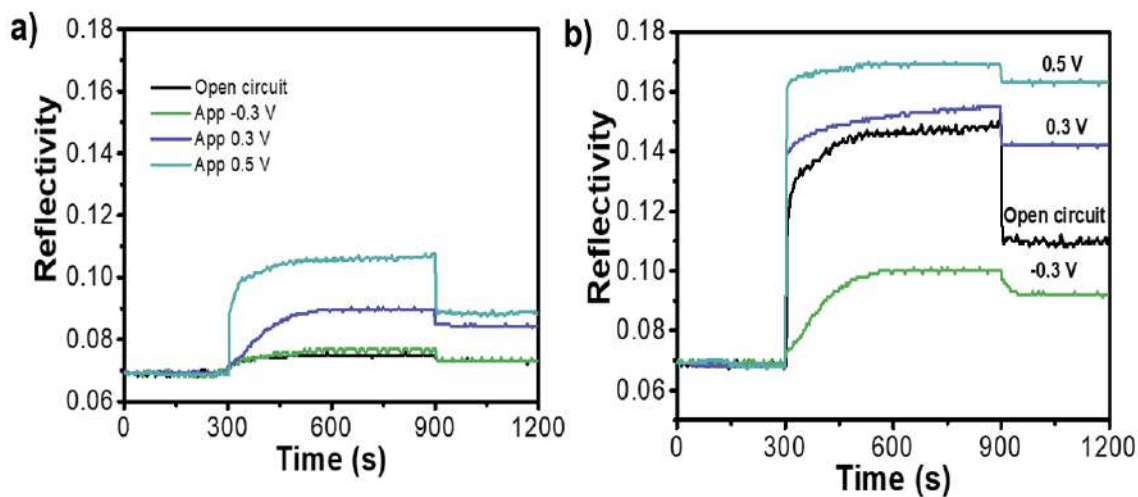


Figure 4.6 (a) SPR curve of AgNPs and AgNPs/creatinine at used electrochemical control of 0.5, 0.3, -0.3 V, and without applied constant potential.

**Table 4.2**  $k_a$  and  $k_d$  provided under electrochemical control of the designed Ppy/aggregated AgNPs-based sensor in the concentration of 0.5 mM creatinine.

Applied potential (V)	$k_a$ ( $M^{-1} s^{-1}$ )	$k_d$ ( $s^{-1}$ )	$K_A$ ( $M^{-1}$ )
Open circuit	$1.53 \times 10^2$	$3.49 \times 10^{-3}$	$4.38 \times 10^4$
-0.3	$4.81 \times 10$	$4.95 \times 10^{-3}$	$9.72 \times 10^3$
0.3	$1.01 \times 10^2$	$6.22 \times 10^{-3}$	$1.62 \times 10^4$
0.5	$3.87 \times 10^2$	$7.39 \times 10^{-3}$	$5.24 \times 10^4$

#### 4.4 CONCLUSION

The EC-SPR technique detects creatinine through using starch/AgNP, which interact specifically and sensitively with creatinine. The linear dynamic range of the developed SPR sensor is 10 to 1000 M. The performance of a creatinine sensor is compared using SPR sensor structures with and without AgNP, as well as before and after aggregated AgNP. Therefore, as compared to the SPR creatinine sensor without AgNP aggregation, the SPR creatinine sensor with AgNP aggregation is about four times more sensitive, with a detection limit of 0.19 M. The sensor created in this study has a great potential for use in the detection of creatinine.

#### 4.5 REFERENCES

- [1] H.H. Nguyen, J. Park, S. Kang, M. Kim, Surface plasmon resonance: a versatile technique for biosensor applications, *Sensors*, 15(2015) 10481-10510.
- [2] S. Mariani, M. Minunni, Surface plasmon resonance applications in clinical analysis, *Analytical and bioanalytical chemistry*, 406(2014) 2303-2323.
- [3] S. Lopez-Giacoman, M. Madero, Biomarkers in chronic kidney disease, from kidney function to kidney damage, *World Journal of Nephrology*, 4(2015) 57-73.
- [4] S. Gowda, P.B. Desai, S.S. Kulkarni, V.V. Hull, A.A.K. Math, S.N. Vernekar, Markers of renal function tests, *North American Journal of Medical Sciences*, 2(2010) 170-173.
- [5] Y. Tonomura, M. Matsubara, I. Kazama, Biomarkers in urine and use of creatinine, in: V.R. Preedy, V.B. Patel, *General Methods in Biomarker Research and their Applications*, Springer Netherlands, Dordrecht, 2015, 165-186.
- [6] P.S. Menon, F.A. Said, G.S. Mei, D.D. Berhanuddin, A.A. Umar, S. Shaari, et al., Urea and creatinine detection on nano-laminated gold thin film using Kretschmann-based surface plasmon resonance biosensor, *PloS one*, 13(2018) e0201228-e.
- [7] S.S. Hinman, K.S. McKeating, Q. Cheng, Surface plasmon resonance: Material and Interface Design for Universal Accessibility, *Analytical chemistry*, 90(2018) 19-39.



## CHAPTER 5

### CONCLUSION

SPR biosensors have been used to detect changes in biological and chemical samples. We believe that the efficiency of SPR biosensor technology will remain to improve. Combining an enhanced SPR sensing platform with novel biospecific surfaces that are highly resistant to nonspecific binding results in a strong SPR biosensor capable of detecting biological and chemical analytes in complex samples in a rapid, sensitive, and specific manner. SPR based on P2ABA/GO is developed for detection of human IgG. GO composited with 2-ABA is electrodeposited on gold surface by CV with a potential range of -0.2 to 1.1 V. for 2 cycles at the scan rate of 20 mV/s. At the same condition, the sensitivity of P2ABA/GO immunosensor is 1.4 folds higher than when GO is not used. These data imply that GO can help the SPR immunosensor detect IgG levels. Electrochemical techniques coupling with SPR spectroscopy promises to generate a novel and effective molecular recognition technology, especially in the purpose for enhancing analytical signal. The EC-SPR immunosensor based on electrodeposited GO/PEDOT/PSS film is successfully developed for the assay of human IgG with electrochemically controlled. In the PBS solution, GO/PEDOT/PSS exhibits electrical activity. CV is employed for electropolymerization on a gold-coated high refractive index glass slide. The -COOH group on the surface of the GO/PEDOT/PSS platform is activated to make ester groups, which are subsequently added to functionalized anti-human IgG. The developed immunosensor can detect human IgG under a variety of constant applied potentials. By measuring in situ EC-SPR, the kinetic feature of

electropolymerization and anti-human IgG/human IgG interaction are measured. After injecting IgG onto the immobilized surface, reflectivity increases, indicating that IgG is interacting with anti-IgG. The response for the kinetics of the reflectivity change after the increased number of binding of human IgG and anti-IgG. In an electrochemical control system with a potential of 0.5 V, human IgG has a greater binding capacity. When using the Freundlich adsorption model, it can be determined that human IgG enhances heterogeneity or electrochemically produced heterogeneity on the surface of the immunosensor. According to these findings, the CP-based EC-SPR sensor has a configurable surface shape and is a sensitive instrument for enhancing molecular biology interaction.

TSPR is a type of optical transmission that is more transparent at wavelengths that are more precise than classical theory technique. Diffraction gratings, nano-hole arrays, and nano-needle arrays are three essential plasmonic structures that enable this phenomenon. The impact of the surface plasmon's excitation causes this unique optical transmission phenomenon. When the dielectric environment of the metal film surface changes, TSPR's reaction varies. Selectivity, sensitivity, and dynamic range of immunosensor have all been improved using TSPR. For the studies of TSPR sensor, we are successful developed the GO for the determination of human IgG. The TSPR spectra of GO/gold grating substrate revealed dominant peaks with light incidence angles ranging from 0° to 40°. The kinetic reaction of TSPR based GO/gold-coated grating pattern could be applied to measure the immunoassay's construction. The binding of IgG and anti-IgG causes a change in TSPR intensity. In comparison to 11-MUA on a gold-coated grating platform, GO on a gold-coated grating

substrate gives higher sensitivity for human IgG testing. This method has the potential to enhance the sensitivity and LOD of TSPR immunosensor devices.

The TSPR-i method, which is based on the use of propagating SPR, is used to monitor changes in surface plasmon resonance of gold grating substrates to their surroundings in transmission mode. For the detection of creatinine, AgNPs are deposited layer-by-layer on gold thin film grating/substrate surfaces utilizing PDADMAC/PSS. A camera connected to LCTF detects the TSPR-i signal. When incubated with creatinine for 1 hour after deposition of AgNPs on the gold grating substrate, the TSPR-i intensity dropped and then increased. On the TSPR imaging system, a simple approach for real-time and label-free imaging is presented, which might be beneficial in clinical applications.

In addition, utilizing the SPR technique, a novel method for creatinine assay utilizing starch-AgNPs on PPy/gold substrate is constructed. The study provides a clear change in the color of AgNPs solution with creatinine, indicating high sensitivity caused by AgNPs' localized plasmon effect. The binding of AgNPs with creatinine on the PPy structure increases the shift of SPR reflectivity based on the Kretschmann configuration. The SPR reflectivity improved with increasing creatinine intensity after injection of the mixture creatinine/AgNPs on the PPy/gold film. The creatinine sensor's performance is compared to that of different SPR sensor platforms: PPy film, PPy/AgNPs, and PPy/aggregated-AgNPs. When compared to a substrate without aggregated AgNPs, the SPR sensor with aggregated AgNPs improves by almost 4 folds, and the LOD is 0.19  $\mu\text{M}$ . The suggested technique has the potential to be great in clinical practice.

## APPENDICE

### Freundlich and Langmuir models for the kinetic study

Association process

$$R_t = R_{eq}\{1 - \exp[-(k_a C + k_d)t]\} \quad (1)$$

where  $R_t$  and  $R_{eq}$  are the reflectivity responses at certain time ( $t$ ) and equilibrium point, respectively.  $k_a$  and  $k_d$  are the association and dissociation rate constants, respectively.

Dissociation process (at  $C = 0$ )

$$R_t = R_{eq}\exp(-k_d t) \quad (2)$$

At equilibrium

$$K_A = k_a/k_d \quad (3)$$

where  $K_A$  is equilibrium association constant.

Freundlich model

$$q = F_F C_e^n \quad (4)$$

where  $q$  and  $C_e^n$  are the shift of reflectivity and the target molecule concentration.  $K_F$  and  $n$  are the Freundlich constants. Equation (4) can be rearranged into a linear form as

$$\log g = \log K_F + n \log C_e \quad (5)$$

## LIST OF PUBLICATIONS

- 1) Chammari Pothipor, Chutiparn Lertvachirapaiboon, Kazunari Shinbo, Keizo Kato, Futao Kaneko, Kontad Ounnunkad\*, and Akira Baba\*\*, “Detection of creatinine using silver nanoparticles on a poly(pyrrole) thin film-based surface plasmon resonance sensor”, Japanese Journal of Applied Physics, Vol. 59, Published: 28 November 2019, SCCA02.
- 2) Chammari Pothipor, Chutiparn Lertvachirapaiboon, Kazunari Shinbo, Keizo Kato, Futao Kaneko, Kontad Ounnunkad\*, and Akira Baba\*\*, “Development of graphene oxide/poly(3,4ethylenedioxythiophene)/poly(styrene sulfonate) thin film-based electrochemical surface plasmon resonance immunosensor for detection of human immunoglobulin G”, Japanese Journal of Applied Physics, Vol. 57, Published: February 2018, 02CA07.
- 3) Chammari Pothipor, Chutiparn Lertvachirapaiboon, Kazunari Shinbo, Keizo Kato, Futo Kaneko, Kontad Ounnunkad\*, and Akira Baba\*\*, “Transmission Surface Plasmon Resonance Imaging based on Gold Grating/Silver Nanoparticles for Detection of Creatinine”, Conference Proceedings of ISEIM, IEEE, Published: December 2017.
- 4) Chutiparn Lertvachirapaiboon, Chammari Pothipor, Kazunari Shinbo, Keizo Kato, Futao Kaneko, Kontad Ounnunkad\*, and Akira Baba\*\*, “Transmission surface plasmon resonance image detection by a smartphone camera”, MRS Communications, Vol. 8, Published: September 2018, 3.

## PRESENTATIONS

- 1) Chamari Pothipor, Rawiwan Laocharoensuk, Jaroon Jakmune, Kontad Ounnunkad\*, Label-Free Electrochemical Human IgG Immunosensor Based on a Screen-Printed Carbon Electrode Modified with Poly(3-aminobenzoic acid)-MWCNT Nanocomposite Film, The 5<sup>th</sup> International Symposium on Organic and Inorganic Electronic Materials and Related Nanotechnologies (*EM-NANO 2015*) TICC June 16-19, 2015. Niigata, Japan. (Poster presentation)
- 2) Chammari Pothipor, Kontad Ounnunkad, Chutiparn Lertvachirapaiboon, Kazunari Shinbo, Keizo Kato, Futao Kaneko, Akira Baba\*, “Improving Surface Plasmon Resonance Immunosensor Based on Graphene Oxide/PEDOT/PSS Film”, The 63<sup>rd</sup> Japan Society of Applied Physics (JSAP 2016), March 19-22, 2016, Tokyo, Japan. (Poster presentation)
- 3) Chammari Pothipor, Kontad Ounnunkad, Chutiparn Lertvachirapaiboon, Kazunari Shinbo, Keizo Kato, Futao Kaneko, Akira Baba\*, “Enhancing Surface Plasmon Resonance Immunosensor Based on GPO/PEDOT-PSS/Cys/GPO Film for human IgG detection”, The 9<sup>th</sup> International symposium on organic molecular electronics (ISOME 2016), May 18-20, 2016, TOKIMATE, Niigata, Japan. (Poster presentation)
- 4) Chammari Pothipor, Kontad Ounnunkad, Chutiparn Lertvachirapaiboon, Kazunari Shinbo, Keizo Kato, Futao Kaneko, Akira Baba\*, “Electrochemical-Surface Plasmon Resonance-Based Immunosensor on Poly(2-aminobenzylamine)/Graphene oxide Nanocomposite Film” The KJF International

Conference on Organic Materials for Electronics and Photonics (KJF-ICOMEF 2016), September 4-7, 2016, ACROS, Fukuoka, Japan. (Poster presentation)

- 5) Chammari Pothipor, Kontad Ounnunkad, Chutiparn Lertvachirapaiboon, Kazunari Shinbo, Keizo Kato, Futao Kaneko, Akira Baba\*, “Sensitivity Enhancement of Electrochemical-Surface Plasmon Resonance IgG Immunosensor Based on Graphene Oxide/Poly(2-Aminibenzylamine) Film”, The 77<sup>th</sup> Japan Society of Applied Physics (JSAP 2016) Autumn meeting, 2016, September 13-16, 2016, TOKI MESSE, Niigata, Japan. (Poster presentation)
- 6) Chammari Pothipor, Kontad Ounnunkad, Chutiparn Lertvachirapaiboon, Kazunari Shinbo, Keizo Kato, Futao Kaneko, Akira Baba\*, “An in Situ Electrochemical-Surface Plasmon Resonance Detection of Human IgG Immunosensor Based on Graphene Oxide/Poly(2-Aminobenzylamine) Film”, JSAP Hokuriku Shinetsu Chapter, December 10, 2016, Toyama, Japan. (Oral presentation)
- 7) Chammari Pothipor, Kontad Ounnunkad, Chutiparn Lertvachirapaiboon, Kazunari Shinbo, Keizo Kato, Futao Kaneko, Akira Baba\*, Transmission Surface Plasmon Resonance Imaging of Gold Grating and Silver Nanoparticle for Creatinine Detection, The 64<sup>th</sup> JSAP spring meeting 2017, March 14-17, 2017, Pacifico, Yokohama, Japan. (Poster presentation)
- 8) Chammari Pothipor, Kontad Ounnunkad, Chutiparn Lertvachirapaiboon, Kazunari Shinbo, Keizo Kato, Futao Kaneko, Akira Baba\*, Development of Graphene Oxide-poly(3,4-ethylenedioxythiophen)/poly(styrenesulfonate) Thin

Film-Based Electrochemical-Surface Plasmon Resonance Immunosensor, The 6<sup>th</sup> International Symposium on Organic and Inorganic Electronic Materials and Related Nanotechnology, June 18-21, 2017, Aossa, Fukui, Japan. (Oral presentation)

- 9) Chammari Pothipor, Kontad Ounnunkad, Chutiparn Lertvachirapaiboon, Kazunari Shinbo, Keizo Kato, Futao Kaneko, Akira Baba\*, Detection of Creatinine Using Silver Nanoparticles on Poly(pyrrole) Thin Film-Based Surface Plasmon Resonance Sensor, 2017 KJF International Conference on Organic Materials for Electronics and Photonics (KJF-ICOMEF 2017), August 30-September 02, 2017, Gwangju, Korea. (Poster presentation)
- 10) Chammari Pothipor, Kontad Ounnunkad, Chutiparn Lertvachirapaiboon, Kazunari Shinbo, Keizo Kato, Futao Kaneko, Akira Baba\*, Transmission Surface Plasmon Resonance Imaging based on Gold Grating/Silver Nanoparticles for Detection of Creatinine, 8<sup>th</sup> International Symposium on Electrical Insulating Materials, September 12-15, 2017, Toyohashi Chamber of Commerce & Industry, Toyohashi City, Japan. (Oral presentation)



## CURRICULUM VITAE

**Author's Name** Miss Chammari Pothipor

**Date/Year of Birth** 15 May 1989

**Place of Birth** Lamphun Province, Thailand

### Education

- 2016-2021 Ph.D. (Electrical and Electronic Engineering)  
Graduate School of Science and Technology Doctoral  
Program of Electrical and Information Engineering  
Electrical and Electronic Engineering, Niigata  
University, Japan
- 2015- 2021 Ph.D. (Chemistry)  
Department of Chemistry, Faculty of Science, Chiang  
Mai University, Thailand
- 2012-2014 M.S. (Chemistry)  
Department of Chemistry, Faculty of Science, Chiang  
Mai University, Thailand
- 2008-2012 B.S. (Biochemistry and Biochemical Technology)  
Department of Chemistry, Faculty of Science, Chiang  
Mai University, Thailand

## **Scholarships**

1. Ph. D. research supported by the Graduate School, Chiang Mai University Thailand (2019)
2. Thailand Graduate Institute of Science and Technology: TGIST, NSTDA, Thailand (2018-2020)

## **Publications**

1. C. Pothipor, J. Jakmune, S. Bamrungsap, K. Ounnunkad, “Dual label-free electrochemical biosensor for simultaneous detection of breast cancer-related microRNA-21 and CA 15-3 based on gold nanoparticles-dyes deposited on a poly(3-aminobenzylamine)/2D-MoSe<sub>2</sub>/graphene oxide film”, *Bioelectrochemistry*, submitted: 3 June 2021.
2. C. Pothipor, J. Jakmune, S. Bamrungsap, K. Ounnunkad, “Electrochemical biosensor for simultaneous detection of breast cancer clinically related microRNAs based on a gold nanoparticles/graphene quantum dots/graphene oxide film”, *Analyst*, 146, 4000-4009, 2021.
3. C. Pothipor, N. Aroonyadet, S. Bamrungsap, J. Jakmune, K. Ounnunkad, “A highly sensitive electrochemical microRNA-21 biosensor based on intercalating methylene blue signal amplification and a highly dispersed gold nanoparticles/graphene/polypyrrole composite”, *Analyst*, 146, 2679-2688, 2021.
4. C. Pothipor, C. Lertvachirapaiboon, K. Shinbo, K. Kato, F. Kaneko, K. Ounnunkad, A. Baba, “Detection of creatinine using silver nanoparticles on a poly(pyrrole) thin film-based surface plasmon resonance sensor”, *Japanese Journal of Applied Physics*, 59, SCCA02, 2019.

5. C. Pothipor, N. Wiriyakun, T. Putnin, A. Ngamaroonchot, J. Jakmune, K. Ounnunkad, R. Laocharoensuk, N. Aroonyadet, “Highly sensitive biosensor based on graphene-poly (3-aminobenzoic acid) modified electrodes and porous-hollowed-silver-gold nanoparticle labelling for prostate cancer detection”, *Sensor and Actuators B-Chemical*, 296, 2019.
6. C. Pothipor, C. Lertvachirapaiboon, K. Shinbo, K. Kato, F. Kaneko, K. Ounnunkad, A. Baba, “Development of graphene oxide/poly(3,4ethylenedioxythiophene)/poly(styrene sulfonate) thin film-based electrochemical surface plasmon resonance immunosensor for detection of human immunoglobulin G”, *Japanese Journal of Applied Physics*, 57, 02CA07, 2018.
7. C. Pothipor, C. Lertvachirapaiboon, K. Shinbo, K. Kato, F. Kaneko, K. Ounnunkad, A. Baba, “Transmission surface plasmon resonance imaging based on gold grating/silver nanoparticles for detection of creatinine”, *Conference Proceedings of ISEIM, IEEE*, 2017.
8. C. Pothipor, N. Kungwan, J. Jakmune, K. Ounnunkad, “A disposable and flexible graphene electrode fabricated by inkjet printing of aqueous surfactant-free graphene oxide dispersion”, *Chemistry Letters*, 44, 6, 2015.
9. S. Chanarsa, C. Pothipor, N. Kungwan, K. Ounnunkad, “A poly(pyrrole-3-carboxylic acid) thin film modified screen printed carbon electrode as highly sensitive and selective label-free electrochemical immunosensing platform”, *Chiang Mai Journal of Science*, 47, 3, 2020.
10. C. Lertvachirapaiboon, C. Pothipor, K. Shinbo, K. Kato, F. Kaneko, K. Ounnunkad, A. Baba, “Transmission surface plasmon resonance image detection by a smartphone camera”, *MRS Communications*, 8, 3, 2018.

## **Awards**

1. Poster Presentation Award, in The Technical Presentation and Innovation of Science Bachelor's Degree, Chiang Mai, February 2012.
2. Travel Award for SOKENDAI Asian Winter School, Graduate University for Advanced Studies (SOKENDAI) and Institute for Molecular Science (IMS), Okazaki, Japan, December 10-13, 2013.
3. Japanese Government (Monbukagakusho) Scholarship program: for research student, Niigata University, Japan (2015-2016)